Characterization of humoral and SARS-CoV-2 specific T cell responses in people living with HIV

Aljawharah Alrubayyi
University of Oxford
Ester Gea-Mallorquí
University of Oxford
Emma Touizer
University College London https://orcid.org/0000-0002-7164-8555
Dan Hameiri-Bowen
University of Oxford
Jakub Kopycinski
University of Oxford
Bethany Charlton
University of Oxford
Natasha Fisher-Pearson
University of Oxford
Luke Muir
University College London
Annachiara Rosa
The Francis Crick Institute https://orcid.org/0000-0001-7433-6357
Chloë Roustan
The Francis Crick Institute
Christopher Earl
The Francis Crick Institute https://orcid.org/0000-0002-9091-9955
Peter Cherepanov
The Francis Crick Institute https://orcid.org/0000-0002-0634-538X
Pierre Pellegrino
Mortimer Market Centre
Laura Waters
Mortimer Market Centre
Fiona Burns
Institute for Global Health UCL
Sabine Kinloch
Royal Free London NHS Foundation Trust
Tao Dong

University of Oxford
Lucy Dorrell
University of Oxford
Sarah Rowland-Jones
https://orcid.org/0000-0001-5788-6998
Laura McCoy
University College London https://orcid.org/0000-0001-9503-7946
Dimitra Peppa (dimitra.peppa@ndm.ox.ac.uk)
University of Oxford

Article

Keywords: SARS-CoV-2, vaccine effectiveness, immunology, antibodies

Posted Date: March 17th, 2021

DOI: https://doi.org/10.21203/rs.3.rs-309746/v1

Version of Record: A version of this preprint was published at Nature Communications on October 5th, 2021. See the published version at https://doi.org/10.1038/s41467-021-26137-7.

Characterization of humoral and SARS-CoV-2 specific T cell responses in people living with HIV

Aljawharah Alrubayyi[1]†, Ester Gea-Mallorquí[1]†, Emma Touizer[2]†, Dan Hameiri-Bowen[1], Jakub Kopycinski[1], Bethany Charlton[1], Natasha Fisher-Pearson[1], Luke Muir[2], Annachiara Rosa[3], Chloe Roustan[3], Christopher Earl[3], Peter Cherepanov[3], Pierre Pellegrino[4], Laura Waters[4], Fiona Burns[5,6], Sabine Kinloch[6], Tao Dong[1], Lucy Dorrell[1], Sarah Rowland-Jones[1], Laura E. McCoy[2]†*, Dimitra Peppa[1,4]†*

Affiliations:

[1] Nuffield Dept of Clinical Medicine, University of Oxford, United Kingdom

[2] Division of Infection and Immunity, University College London, London, United Kingdom

[3] Chromatin Structure and Mobile DNA Laboratory, The Francis Crick Institute, London, United Kingdom

[4] Mortimer Market Centre, Department of HIV, CNWL NHS Trust, London, United Kingdom

[5] Institute for Global Health UCL, London, United Kingdom

[6] Royal Free London NHS Foundation Trust, London, United Kingdom

† These authors contributed equally

Corresponding authors: Dimitra.peppa@ndm.ox.ac.uk; l.mccoy@ucl.ac.uk

One Sentence Summary: Adaptive immune responses to SARS-CoV-2 in the setting of HIV infection

Abstract

There is an urgent need to understand the nature of immune responses against SARS-CoV-2, to inform risk-mitigation strategies for people living with HIV (PLWH). We show that the majority of PLWH, controlled on ART, mount a functional adaptive immune response to SARS-CoV-2. Humoral and SARS-CoV-2-specific T cell responses are comparable between HIV-positive and negative subjects and persist 5-7 months following predominately mild COVID-19 disease. T cell responses against Spike, Membrane and Nucleocapsid are the most prominent, with SARS-CoV-2-specific CD4 T cells outnumbering CD8 T cells. We further show that the overall magnitude of SARS-CoV-2-specific T cell responses relates to the size of the naive CD4 T cell pool and the CD4:CD8 ratio in PLWH, in whom disparate antibody and T cell responses are observed. These findings suggest that inadequate immune reconstitution on ART, could hinder immune responses to SARS-CoV-2 with implications for the individual management and vaccine effectiveness in PLWH.

Introduction

The global outbreak of severe acute respiratory syndrome coronavirus 2 (SARS-CoV-2), causing COVID-19 disease, has resulted in an overall 3% case fatality rate, posing unprecedented healthcare challenges around the world [1]. With an evolving pandemic, urgent and efficient strategies are required for optimised interventions especially in patient populations with underlying chronic diseases. Nearly 40 million people are living with HIV (PLWH) worldwide and almost half of PLWH in Europe are over the age of 50 [2]. However, due to scarcity of data it remains unknown whether antiviral responses to SARS-CoV-2 are compromised and/or less durable in PLWH following primary infection. Such knowledge is crucial in the future clinical management

of PLWH during the course of the pandemic and for informing strategies for vaccination programmes.

Epidemiological evidence indicates that the risk of severe COVID-19 disease increases with age, male gender, and in the presence of comorbidities [3,4]. PLWH, despite efficient virological suppression on antiretroviral treatment (ART), experience an increased burden of comorbid conditions associated with premature ageing [5,6]. These multi-morbidities are driven by residual inflammation on ART and ongoing immune dysregulation [7] that could influence COVID-19 disease severity, the durability of protective antiviral responses, which may prevent future re-infection, and responsiveness to vaccination [8,9]. Although there is no evidence of increased rates of COVID-19 disease among PLWH compared to the general population, mortality estimates vary between studies, with disparities in social health determinants and comorbidities likely having an influence [10-16]. More recently, cellular immune deficiency and a lower CD4 T cell count/low CD4 T cell nadir have been identified as potential risk factors for severe SARS-CoV-2 infection in PLWH, irrespective of HIV virological suppression [17]. Burgeoning evidence supports a role for CD4 T cells in the control and resolution of acute SARS-CoV-2 infection [18-20], in addition to providing CD8 T cell and B cell help for long-term immunity [21-22]. Any pre-existing CD4 T cell depletion in PLWH, as described in patients with haematological malignancy [23], could therefore be a potential driver of dysregulated immunity to SARS-CoV-2, hampering antiviral responses [24] and development of immunological memory.

Despite the collective efforts to define the correlates of immune protection and evaluate the durability of protective immune responses elicited post SARS-CoV-2 infection in the general

70 population, reports in PLWH are limited. Overall, the majority of people infected with SARS-
71 CoV-2 in the absence of HIV develop durable antibody responses including neutralizing antibodies
72 and T cell responses [18,25-28]. In most cases the magnitude of humoral responses is complemented
73 by multi-specific T cell responses and appears to be dependent on the severity and protracted
74 course of COVID-19 disease [18,27,29]. However, humoral and cellular immune responses are not
75 always correlative, with T cell immunity being induced even in the absence of detectable
76 antibodies during mild COVID-19 disease [18,30-31] and predicted to be more enduring from
77 experience with other coronaviruses [32-33]. Notably, older individuals more often display poorly co-
78 ordinated immune adaptive responses to SARS-CoV-2 associated with worse disease outcome
79 [18,34]. This is particularly pertinent for PLWH, in whom the combined effect of ageing/premature
80 immunosenescence and residual immune dysfunction in the era of effective of ART could have
81 important consequences for the development of immune responses to a new pathogen and
82 vaccination [35]. To date, a single case report suggests a longer disease course and delayed antibody
83 response against SARS-CoV-2 in HIV patients [36], but a simultaneous assessment of antibodies and
84 T cell responses in the convalescent phase of COVID-19 disease is lacking in PLWH.
85
86 To address this knowledge gap, we performed an integrated cross-sectional analysis of different
87 branches of adaptive immunity to SARS-CoV-2 in PLWH, controlled on ART, compared to HIV
88 negative individuals recovered from mainly non-hospitalized mild COVID-19 disease. Our data
89 reveal an association between the magnitude of SARS-CoV-2 T cell responses and the CD4:CD8
90 ratio in PLWH, in whom a decreased representation of naïve CD4 T cell subsets could potentially
91 compromise protective immunity to SARS-CoV-2 infection and/or vaccination.
92

Results

COVID-19 cohort

Forty-seven individuals with HIV infection, well controlled on ART (for >2 years) with an undetectable HIV RNA, were recruited for this study during a defined period of time between July 2020 and November 2020. Of these donors, twenty four previously had laboratory confirmed SARS-CoV-2 diagnosis (RT-PCR+ and/or Ab positive) with a median days post-symptom onset (DPSO) of 148 days; twenty three were probable/possible cases with a higher median DPSO of 181 days. The majority had ambulatory mild COVID-19 disease not requiring hospitalization (score 1-2 on WHO criteria). Eight subjects out of the laboratory confirmed cases had moderate disease requiring hospitalization (score 4-5 on WHO criteria). The ages of the subjects ranged from 30-73 years of age (median 52 years old) and were predominately White Caucasian males. The cohort included donors capturing a range of CD4 counts (133-1360) and CD4:CD8 ratios (0.17-2.54), reflective of the different lengths of HIV infection/CD4 T cell nadir and variable levels of immune reconstitution post treatment. As a comparator group we sampled thirty five HIV seronegative health care workers (HCW), thirty one with laboratory confirmed SARS-CoV-2 diagnosis and four suspected/household contacts of a confirmed case. The HCW group had a mild course of COVID-19 disease sampled at a similar median DPSO, with four donors recruited in the convalescent phase post moderate disease (score 4-5 on WHO criteria). HIV negative subjects were younger in age (range 26-65; median 41) with a more equal female:male distribution (**Supplementary Table 1**). A group of HIV positive (n=16) donors with samples stored prior to the pandemic, matched to the HIV cohort recovered from COVID-19 disease, was used as controls. Inter-experimental variability was minimized by running matched cryopreserved samples in

batches with inter-assay quality controls. Further details on patients' characteristics and comorbidities are included in **Supplementary Table 1**.

Levels of SARS-CoV-2 antibodies in the study groups

ELISA was used to screen plasma samples for antibodies against the external Spike antigen, using immobilized recombinant Spike $S1_{1-530}$ subunit protein (S1), and against immobilized full-length internal Nucleoprotein (N) antigen to confirm prior infection as previously described [33,37,38] (**Fig.1a**). A sample absorbance greater than 4-fold above the average background of the assay was regarded as positive, using a threshold established with pre-pandemic samples (**Supplementary Fig.1a, b**) and as previously described [38]. The screening assay, followed by titer quantification (based on an in-assay standard curve) [37], demonstrated that 95.8% (23/24) of individuals from the HIV positive group with prior laboratory confirmed COVID-19 and 30.43% (7/23) with suspected disease, during the first wave of the pandemic, had measurable titers for SARS-CoV-2 S1 and N sampled at a median 146 DPSO (DPSO range 46-232) and 181 DPSO (range 131-228), respectively (**Fig.1a-c**). Similarly, in the HIV negative group with laboratory confirmed COVID-19 disease, 93.5% (29/31) had detectable SARS-CoV-2 antibodies to S1 and N at 146 DPSO (101-220), whereas none of the suspected/household contacts in this group (0/4) had quantifiable titers (DPSO median 200; range 125-203) (**Fig.1a-c**). S1 and N titers were found to be comparable between the HIV positive and negative groups (**Fig.1b, c**) and correlated with one another, although levels were heterogenous among donors as previously observed (**Fig.1d**).

To determine whether the SARS-CoV-2 antibodies generated are able to inhibit SARS-CoV-2 infection, we employed a serum neutralisation assay with pseudotyped SARS-CoV-2, to calculate

the 50% inhibitory serum dilution (ID50) [28]. Overall, we detected similar neutralization levels (**Fig.1e**) and comparable profiles across the two study groups in terms of the number of individuals with high potency, low potency or no neutralizing activity (<50 ID50) (**Fig.1f**), which correlated with anti-S1 IgG levels (**Fig.1g**). A range of neutralizing antibodies (nAb) was detected in the groups, with some samples exhibiting strong neutralization despite low S1 titers irrespective of disease severity (**Fig.1g**).

No association was observed between S1 binding titers, age and gender in the two groups (**Supplementary Fig.1c**). A weak positive correlation was seen between neutralization levels and age according to male gender in the HIV positive group, where subjects were older and females were notably under-represented (**Supplementary Fig.1d**). Neutralization levels did not correlate with DPSO (**Supplementary Fig.1e**) and were detectable up to 7 months post infection. No clear association was observed according to ethnicity (**Supplementary Fig.1f**). Together these results show no significant differences in the IgG-specific antibody response to SARS-CoV-2 and neutralization capacity according to HIV status after recovery from COVID-19 disease. These findings should be considered in the context of this cohort in which the majority of cases were mild and therefore may not reflect the full burden of disease associated with SARS-CoV-2 infection.

SARS-CoV-2 multi-specific T cell responses

The presence of T helper 1 (Th1) immunity has been described in a number of studies investigating T cell-specific immune responses to SARS-CoV-2 infection in various phases of the infection. We therefore initially assessed global SARS-CoV-2 T cell frequencies by IFN-γ-ELISpot using

161 overlapping peptide (OLP) pools to detect T cell responses and cumulative frequencies directed
162 against defined immunogenic regions, including Spike, Nucleocapsid (N), membrane (M),
163 Envelope (Env), and open reading frame (ORF)3a, ORF6, ORF7 and ORF8 (**Fig.2a**). Out of the
164 30 HIV positive and 30 HIV negative individuals (including previously laboratory confirmed cases
165 and additional subjects found to be SARS-CoV-2 seropositive on screening), the majority of
166 donors in each group had a demonstrable cellular response directed predominately against Spike
167 and N/M. Responses to accessory peptide pools (ORFs) and the structural protein Env were less
168 frequent and significantly lower to other antigens observed, irrespective of HIV status (**Fig.2b and**
169 **Supplementary Fig.2a, b**). The overall magnitude of responses against Spike, M and N did not
170 differ significantly between the groups (**Fig.2c**). In HIV positive donors the cumulative SARS-
171 CoV-2 responses across all pools tested were lower in magnitude compared to that of T cells
172 directed against well-defined CD8 epitopes from Influenza, Epstein Barr Virus (EBV) and
173 Cytomegalovirus (CMV)-(FEC pools) tested in parallel within the same donors, but higher
174 compared to HIV-gag responses (**Fig.2d**). By contrast, responses to FEC pools were comparable
175 in magnitude to the cumulative SARS-CoV-2-specific T cell responses detected in the HIV
176 negative donors, likely reflecting the lower CMV seropositivity in the HIV negative group
177 compared to the HIV positive group (54.28% CMV seropositive versus 97.87% CMV seropositive,
178 respectively) (**Fig.2d**). In line with previous studies we observed a wide breadth and range of
179 cumulative SARS-CoV-2 T cell frequencies, with over 90% of donors in each group showing a
180 response (**Fig.2e, f**) [30,39-40]. However, the proportion of HIV positive and negative donors with T
181 cell responses to individual SARS-CoV-2 pools within given ranges varied, with a higher
182 percentage of HIV positive donors having low level responses **(Fig.2g).**
183

Responses to Spike, M and N peptide pools were significantly higher in donors with confirmed SARS-CoV-2 infection compared to subjects with no evidence of infection who displayed relatively weak responses; small responses were also noted in a proportion of HIV positive subjects with available pre-pandemic samples (**Supplementary Fig.2c**). Additional work is required to investigate potential cross-reactive components of these responses with other human coronaviruses, as has been reported in other studies [31-32,39,41]. These data were derived from cryopreserved samples, which may underestimate the magnitude of the detected responses [42].

Given the considerable heterogeneity in the magnitude of the observed responses in both groups, we related these to HIV parameters, age, gender and DPSO. We detected a positive correlation between CD4:CD8 ratio and summed total responses to OLP pools against SARS-CoV-2 in HIV positive subjects (r=0.3820, p=0.037) **(Fig.2h)**; this relationship was similar for N (r=0.4282, p=0.018) and stronger for responses against M (r=0.4853, p=0.007) **(Supplementary Fig.2d, e).** These data suggest that, despite effective ART, incomplete immune reconstitution may potentially impact on the magnitude of T cell responses to SARS-CoV-2. Previous observations have demonstrated an association between SARS-CoV-2-specific T cells, age and gender, with T cell immunity to Spike increasing with age and male gender in some studies [30]. Despite an older age and male predominance in our HIV cohort we did not detect any association between ELISpot responses to Spike and donor age (**Supplementary Fig.2f, g**). There was no correlation between DPSO and T cells directed either against Spike or total responses against SARS-CoV-2. These responses were nonetheless detectable up to 232 DPSO (median 151 range 46-232) in HIV positive subjects, and similarly in HIV negative donors (median 144; range 101-220) (**Supplementary Fig.2h, i**). Given that the majority of the donors, in both groups, experienced mild COVID-19

disease, any associations between the magnitude of responses and disease severity are limited. No differences were observed in the magnitude of T cell responses according to ethnicity and gender, irrespective of HIV status (**Supplementary Fig.2j, k**).

T cell and antibody response complementarity

Next, we compared T cell responses, antibody levels and nAb responses in individual donors to better understand any complementarity between humoral and cellular responses detected by IFN-γ-ELISpot. SARS-CoV-2-specific T cell responses correlated with antibody binding titers in the HIV negative group (**Fig.3a, c**). Although the majority of HIV positive subjects had detectable antibody and T cell responses to SARS-CoV-2, the magnitude of the cellular immune responses correlated weakly only with N IgG binding titers but not with S1 IgG binding titers (**Fig.3b, d**). We subsequently examined neutralization ID50 values for individual donors in relation to T cell responses to individual SARS-CoV-2 antigen pools and summed responses. In HIV negative donors a correlation was observed between T cell responses to Spike protein and ID50 ($r= 0.4002$, $p= 0.0315$), with donors lacking a response to Spike generally maintaining low-frequency T cell responses to other specificities. When cumulative responses were ranked by the magnitude of nAb response, a single HIV negative donor with an ID50>1000 had no detectable SARS-CoV-2-specific T cells (**Fig.3e**). In HIV positive donors no correlation was detected between neutralization capacity and responses to individual SARS-CoV-2 peptides or pooled responses. A single HIV positive donor (1/29) with undetectable neutralization activity, and another donor with potent neutralization (>1000), had no measurable T cell response to any of the pools tested (**Fig.3f**).

SARS-CoV-2 specific T cell responses are dominated by CD4 T cells

Following the initial broad screening of the antiviral responses to SARS-CoV-2, intracellular cytokine staining (ICS) was used to assess the composition and polyfunctionality of T cell responses in a group of HIV positive (n=11) and HIV negative (n=12) donors with available PBMC and detectable responses by IFN-γ-ELISpot. To determine the functional capacity of SARS-CoV-2-specific CD4 and CD8 T cells, we stimulated PBMCs with overlapping Spike, M and N (non-Spike) peptide pools, in addition to CMV pp65 and HIV gag peptides within the same individuals. We focused on Spike, M and N as these antigens dominated responses detected by ELISpot. Expression of the activation marker CD154 and production of IFN-γ, IL-2 and TNF-α were measured as functional readouts (**Fig.4a)**. SARS-CoV-2-specific CD4 T cells directed against Spike and non-Spike (M/N) predominantly expressed CD154 alone or in combination with IL-2, TNF-α and IFN-γ, consistent with a Th1 profile, and these aggregated responses were comparable between the groups (**Fig.4a, b**). SARS-CoV-2-specific CD4 T cells exhibited polyfunctional responses, with T cells expressing up to three cytokines (**Fig.4c**). We detected no significant differences in CD4 T cell responses, according to cytokine profile, to individual pools directed against Spike, M and N in the two groups (**Fig.3c and Supplementary Fig.3a**). Aggregated CD4 T cell responses against all SARS-CoV-2 pools tested were higher compared to CMV-specific responses and HIV-gag responses within the same donors (**Supplementary Fig.3d, e**).

SARS-CoV-2-specific CD8 T cells largely expressed IFN-γ alone or in combination with TNF-α, exhibiting a different cytokine profile to CD4 T cells as expected (**Fig.4d**). A trend toward lower mean aggregated CD8 T cell responses and polyfunctionality against Spike relative to non-Spike was observed in HIV negative individuals (**Fig.4e-f**). Although SARS-CoV-2-specific CD8 T cell

responses did not differ significantly between the two groups, mean response frequency was lower in HIV positive individuals against non-Spike pools (**Fig.4e**). When we examined the individual cytokine profile, depending on antigen specificity, IL-2 production was reduced in CD8 T cells targeting non-Spike pools in HIV positive individuals compared to HIV negative donors (**Supplementary Fig.3f-h**). The proportion of CD8 T cells specific for CMV was higher compared to SARS-CoV-2-specific CD8 T cells irrespective of HIV status and similar to HIV-gag responses (**Supplementary Fig.3i, j**). Notably, SARS-CoV-2-specific CD8 T cells against Spike and non-Spike pools were less frequent, with CD4 T cells similarly outnumbering CD8 T cells regardless of HIV status (**Fig.4g**). Total SARS-CoV-2-specific CD4 T cell responses correlated with the magnitude of T cell responses detected by ELISpots and with neutralization titers in the same individuals when data from HIV positive and negative donors were combined **(Fig.4h, i).** This association was also seen between Spike and non-Spike-specific CD4 T cells detected via ICS and overall T cell responses against Spike/non-Spike detected via ELISpots ($r=0.5734$, $p=0.0042$ and $r=0.4852$, $p=0.0189$ respectively), indicating that CD4 T cells are the dominant population responding to SARS-CoV-2.

In line with previous observations, we found that SARS-CoV-2-specific T cells predominately display an effector memory (EM) and/or a terminally differentiated effector memory (TEMRA) cell phenotype for CD4 and CD8 T cells respectively (**Fig.5a-d**) [25,43]. Previous studies have suggested that higher expression of programmed cell death-1 (PD-1) on T cells in COVID-19 patients could signify the presence of exhausted T cells [44-46]. We therefore examined the expression of PD-1 in relation to activation and function among SARS-CoV-2-specific CD4 T cells. The proportion of CD154+ IFN-γ producing cells was significantly higher in PD-1^+ cells compared to

PD-1$^-$ cells regardless of HIV serostatus, likely reflecting activated functional cells rather than exhausted populations (**Fig.5e**) [47]. An inverse correlation between the expression of PD-1 expressing SARS-CoV-2-specific CD4 T cells and DPSO was observed in HIV negative donors (**Fig.5f**).

Immune profile relationships between convalescent HIV positive and negative individuals

During COVID-19 disease, excessive activation of T cells can lead to lymphopenia, including altered subset distribution and function, and these alterations can persist into convalescence [43,44,48,49]. This prompted us to further evaluate changes in the T cell compartment and the relationship between antigen-specific T cells and antibodies with individual T cell parameters and immunological metrics in our cohort. To this end we utilized a broad immunophenotyping flow cytometry panel to capture major cell types.

Global t-distributed stochastic neighbour embedding (t-SNE) high dimensional analysis demonstrated significant alterations in the T cell compartment between HIV negative and positive individuals recovered from COVID-19 (**Fig.6a**). Lower proportions of circulating CD4 T cells and higher proportions of CD8 T cells were confirmed by traditional gating in HIV infected individuals recovered from COVID-19 disease compared to HIV negative individuals (**Fig.6b**). Consistent with alterations described in HIV infection (L. Zhang et al 1999, M.D. Hazenberg et al 2000, D.C. Douek 1998), naïve T cell frequency was reduced in SARS-CoV-2 convalescent HIV positive donors compared to HIV negative subjects. This was accompanied by higher proportions of terminally differentiated effector memory (TEMRA: CD45RA$^+$CCR7$^-$) within the total CD8 T cell population in HIV infected individuals, contributing to an altered representation of

naïve/memory T cells [50] (**Fig.6c**). Notably, the percentage of naïve CD4 T cells correlated with the CD4:CD8 ratio and SARS-CoV-2-specific T cell responses in HIV positive donors (**Fig.6d, e**), suggesting that the scarce availability of naïve CD4 T cells could influence the extent/magnitude of the T cell response to SARS-CoV-2 infection. Recent data have demonstrated a link between naïve CD4 T cells, age and COVID-19 disease severity in older individuals [18]. Whereas naïve CD8 and CD4 T cells correlated with age in HIV negative donors, this relationship between age and naïve T cells was lost in HIV infected donors (**Fig.6f-i**). Together these observations suggest that altered T cell homeostasis and likely premature immunosenescence in HIV infection could compromise T cell mediated responses to a new pathogen [51].

HIV infection is characterised by persistent immune activation together with cell alterations and T cell exhaustion [52-53]. Although the proportion of T cells co-expressing HLADR/CD38 and PD-1/TIGIT (T cell immunoreceptor with Ig and ITIM domains) in HIV infected individuals was significantly higher when compared with HIV negative donors it did not correlate with SARS-CoV-2-specific parameters (**Supplementary Fig.4a-d).**

Next we assessed circulating T follicular helper (cTfh) cells that represent a substantial proportion of the SARS-CoV-2-specific T cells in acute and convalescent infection [18,54], and are required for maturation and development of B cell responses in germinal centres and the induction of IgG production [21]. A close association between cTfh cells and the virus-specific antibody production in the convalescent phase of COVID-19 disease has been described [55]. We detected elevated frequencies of cTfh (CXCR5+PD-1+) HIV infected subjects compared to HIV infected donors, however, no correlation was observed with antibody levels (**Supplementary Fig.4e, f**). Whether

322 further quantitative and qualitative differences exist between cTfh cell subsets in HIV positive [56]
323 and negative individuals that could alter their capacity to instruct B cells and influence responses
324 to SARS-CoV-2 infection merits further investigation in larger cohorts.
325

326 **Discussion**

327 The COVID-19 pandemic is causing much global uncertainty, especially for people with pre-
328 existing medical conditions such as PLWH. In this study, we aimed to bridge the knowledge gaps
329 in our understanding of the specificity, magnitude and duration of immunity to SARS-CoV-2 in
330 this patient group, which is critical for tailoring current and future mitigation measures, including
331 vaccine strategy. This integrative analysis demonstrates that the majority of PLWH evaluated in
332 the convalescent phase from mild COVID-19 disease can mount a functional adaptive immune
333 response to SARS-CoV-2.
334

335 Most PLWH developed S1/N-reactive and neutralizing antibody responses similar to HIV negative
336 donors in our study and similar to observations reported in the general population at least five
337 months after primary infection [30,57] [28]. Circulating SARS-CoV-2 neutralizing antibody titers were,
338 however, low in a fraction of recovered COVID-19 cases [25,27-29], indicating that either the serum
339 concentration/neutralizing antibody potency was suboptimal or, more likely, that an earlier
340 response could have waned by the time of sampling at DPSO as previously observed [28]. Some
341 samples in both groups showed strong neutralization despite low anti-S1 binding titers, suggesting
342 the possibility of the presence of neutralizing antibodies directed against other viral epitopes and/or
343 greater production of non-neutralizing antibodies, or a role of other isotypes in neutralizing
344 responses. It should be noted that our data reflect those who recovered from mostly mild COVID-

19 disease, limiting our conclusions about disease associations. Whether seroconversion rates and kinetics of antibody responses differ according to HIV status need to be addressed in longitudinal studies from acute infection or vaccination into convalescence. While the exact duration of immunity conferred by natural infection remains unresolved, induction of neutralizing antibodies and presence of antibodies to SARS-CoV-2 is thought to confer a degree of protection against SARS-CoV-2 [58-63].

In addition to antibodies, CD4 T cells and CD8 T cells can provide protective roles in controlling SARS-CoV-2 infection [64,65], with T cell immunity potentially being more enduring, as in the case of SARS-CoV [32,66]. In keeping with the published literature, we detected T cell responses via IFN-γ-ELISpot in the majority of HIV positive and negative donors. In both groups these responses were variable in magnitude and predominately targeted Spike, M and N, with smaller responses to regions of the viral proteome tested being detected, consistent with previous studies [30,39-40].

Notably, a positive association was observed between the CD4:CD8 ratio in HIV infected subjects and the magnitude of T cell responses against SARS-CoV-2. This suggests that some PLWH with residual immune perturbations, despite effective virological suppression on ART, may generate suboptimal T cell memory responses. With emerging information on PLWH with COVID-19 disease, a more pronounced immunodeficiency, defined as a current CD4 count <350/μL and a low CD4 nadir, has been associated with an increased risk for severe COVID-19 disease and mortality. With modern ART and successful viral suppression, absolute CD4 count (despite normalisation) may not accurately reflect the extent of immunological alterations that could persist in HIV infected individuals on treatment [67]. A low or inverted CD4/CD8 ratio is considered an

immune risk phenotype associated with altered immune function, immunosenescence and chronic inflammation in both HIV positive and negative populations [68-70]. Due to its predictive power for adverse clinical outcomes in HIV infection and in the ageing general population [70-72], including its potential role as a prognostic factor of COVID-19 disease severity [24], the CD4:CD8 ratio could represent an additional tool for risk stratification of PLWH. The relationship between naïve CD4 T cells, CD4:CD8 ratio and magnitude of SARS-CoV-2-specific responses in our cohort highlights the dependency between new antigen-specific responses and the available pool of naïve lymphocytes. Fewer pre-existing naïve CD4 T cells coupled with the relative overrepresentation of memory CD8 T cells in the context of HIV, independent of age, could exacerbate the clinical outcome of SARS-CoV-2 infection. These changes in the T cell compartment can lead to reduced priming and poorly coordinated early and subsequent memory immune responses to SARS-CoV-2. Our cohort and interim analysis does not represent the entire spectrum of immune dysfunction, which we will continue to probe through ongoing recruitment to test these relationships more rigorously. This would be highly relevant in the context of emergence of specific SARS-CoV-2 variants associated with immunosuppression described in the UK [73], and in parts of the world with high HIV prevalence and suboptimal HIV suppression levels [74].

In agreement with other studies, our data show that in individuals with detectable cellular responses, CD4 T cell responses to SARS-CoV-2 Spike and non-Spike antigens are more common than CD8 T cell responses [31,39,75]. This could reflect a bias, from using peptide pools, towards MHC class II presentation and more selective recognition by CD4 T cells [39]. Preferential expansion of CD4 T cells has been associated with control of primary SARS-CoV-2 infection [18] underscoring their relevance in PLWH with persistent alterations in their T cell compartments. In a small group

391 of donors, already found to be responsive via ELISpots, further evaluation of T cell
392 polyfunctionality in response to SARS-CoV-2 Spike and non-Spike pools revealed similar profiles
393 in SARS-CoV-2 CD4 T cells irrespective of HIV status. Given that contributions of T cells specific
394 to any viral protein can be relevant for protective immunity, non-Spike proteins could also
395 represent valuable components for future vaccine strategies. The reduced production of IL-2 from
396 SARS-CoV-2-specific CD8 T cells in HIV infected donors could, however, hinder their
397 proliferative potential and long-term immune memory post natural infection and/or immunization
398 [76]. Together, these results provide further immunological context into the described associations
399 between ongoing immunodeficiency and worse COVID-19 disease outcome, and the subsequent
400 development of immune memory responses. Further work is required to comprehensively
401 characterise the epitope repertoire elicited by SARS-CoV-2 infection in the context of a broad set
402 of HLA alleles to define patterns of immunodominance.
403
404 Our data indicate that antibody and T cell responses in convalescent individuals with
405 predominately mild disease can be uncoupled, implying that the binding titer is not always a good
406 predictor of the magnitude of the T cell response, especially in PLWH. The lack of correlation
407 between Spike-specific T cells and S1 binding IgG titers and neutralization levels in HIV positive
408 individuals could point toward impairment of Tfh cells [56], which make up a significant proportion
409 of SARS-CoV-2-specific cells [77,78]. The observed disparity of T cell and antibody responses in
410 certain individuals could also reflect differences in early innate immune responses potentially
411 resulting in dysregulated priming and incongruent T and B cell responses [79]. However, this remains
412 to be determined.
413

There are limitations to this study. The observed heterogeneity in the magnitude of cellular and humoral responses that are not always fully coordinated highlights the need to consider additional putative factors as they relate to adaptive immunity. This cross-sectional study was not powered to study age and demographic differences according to the full spectrum of COVID-19 disease by HIV serostatus. Larger studies are required to determine the role of gender, racial and ethnicity effects, especially in areas of high HIV burden and additional comorbidities, to help identify individuals who are particularly vulnerable to the impact of SARS-CoV-2 infection and need targeted vaccination interventions. Nonetheless, the prospective, longitudinal design of this current study, integrating clinical parameters, antibody and T cell responses, will help address longer term protective immunity and emerging questions, such as immune responses to new SARS-CoV-2 variants [73,74,80-82], and during the subsequent vaccination roll-out.

Collectively, our results provide benchmark data into the facets of adaptive immunity against SARS-CoV-2 in the setting of treated HIV infection, providing evidence for medium-term durable antibody and cellular responses. Although reassuring, our data also have implications for PLWH with inadequate immune reconstitution, reflected in the low/inverted CD4:CD8 ratio, and potentially decreased ability to respond to SARS-CoV-2. This subpopulation of PLWH may be more vulnerable to circulating virus with relevance to vaccine prioritization and potential effectiveness. In the era of ART, CD4:CD8 ratio, should be considered as a readily accessible biomarker for assessing individual risks in PLWH, a proportion of whom may require tailored vaccine strategies to achieve long-term protective immunity.

Materials and Methods

Ethics statement

The protocols for the human study were approved by the local Research Ethics Committee (REC) – Berkshire (REC 16/SC/0265). The study conformed to the Helsinki declaration principles and Good Clinical Practice (GCP) guidelines and all subjects enrolled into the study provided written informed consent.

Study Subjects

HIV seronegative adults (>18 years of age, comprising hospital-based healthcare workers) and chronically HIV infected patients (on antiretroviral treatment for at least 2 years with undetectable HIV RNA) with prior confirmed or suspected COVID-19 disease were recruited. All study participants were screen anti-Hepatitis C virus and anti HBsAg negative. Confirmed SARS-CoV-2 infection by SARS-CoV-2 PCR and/or Roche antibody tests was declared by the participants, who were asked to provide details on the timing and nature of symptoms. Additional demographic information and underlying medical conditions were captured on a health questionnaire. European Centre for Disease Prevention (ECDC) criteria were used for case definition for COVID-19 disease. Severity of COVID-19 disease was according to the WHO criteria. This is a cross-sectional analysis of baseline samples collected during the convalescent phase of SARS-CoV-2 infection as part of a prospective, observational longitudinal cohort study. A total of n=47 HIV positive and n=35 HIV negative subjects with recovered confirmed and/or suspected COVID-19 disease were included (**Supplementary Table 1**). Sixteen demographically age-, sex- and lifestyle-matched HIV-1 seropositive individuals were included for comparison, from whom sample were collected between (February 2017-November 2019; pre-pandemic). All participants were recruited at the Mortimer Market Centre for Sexual Health and HIV Research and the Royal

Free Hospital (London, UK) following written informed consent as part of a study approved by the local ethics board committee. Clinical characteristics of participants are summarized in **Supplementary Table 1**. Further details in the exact number of subjects utilized for each assay are indicated in the figure legends and Results section.

Case definition for coronavirus disease 2019 (COVID-19), as of 03 December 2020 European Centre for Disease Prevention and Control [https://www.ecdc.europa.eu/en/covid-19/surveillance/case-definition]. Severity of COVID-19 was classified according to the WHO (World Health Organisation) clinical progression scale.

Peripheral blood mononuclear cells (PBMC) and Plasma Isolation

Whole blood from all participants was collected in heparin-coated tubes and stored at room temperature prior to processing. In brief, PBMCs were isolated by density gradient sedimentation. Whole blood was transferred to conical tubes and then centrifuged at 2000 rpm, at room temperature (RT) for 5-10 minutes. Plasma was then collected, aliquoted and stored at −80°C for further use. The remaining blood was diluted with RPMI (Corning, Manassas, VA, USA), layered over an appropriate volume of room temperature Histopaque (Histopaque-1077 Cell Separation Medium, Sigma-Aldrich, St. Louis, MO, USA), and then centrifuged for 20 min at 2000 rpm at room temperature without brake. After centrifugation, the PBMC layer was carefully collected, transferred to a conical tube and washed with RPMI. An aliquot of cells was stained with trypan blue and counted using Automated Cell Counter (Bio-Rad, Hercules, California, USA). Isolated PBMCs were then cryopreserved in a cryovial in cell recovery freezing medium containing 10% Dimethyl Sulfoxide (DMSO) (MP Biomedicals, LLC, Irvine, CA, USA) and 90% heat inactivated

fetal bovine serum (FBS) and stored at −80°C in a Mr. Frosty freezing container overnight before being transferred to liquid nitrogen for further storage.

Serum isolation

For serum isolation, whole blood was collected in serum separator tubes and stored briefly at room temperature prior sample processing. Serum tubes were centrifuged for 5 min at 2000 rpm, and then serum was collected, aliquoted and stored at −80°C for further use.

Semiquantitative ELISA for S1 and N

This assay is based on a previously described assay [28,37,38]. Briefly, 9 columns of a 96-half-well Maxisorp plate (Nalgene, NUNC International, Hereford, UK) were coated overnight at 4°C with 25 µl of S1 or N (gift from Peter Cherepanov, Crick Institute) purified protein at 3 µg/ml in PBS, the remaining 3 columns were coated with 25 µl goat anti-human F(ab)'2 (1:1,000) in PBS to generate an internal standard curve. The next day, plates were washed with PBS-T (0.05% Tween in PBS) and blocked for 1h at RT with assay buffer (5% milk powder PBS-T). Assay buffer was then removed and 25 µl of patient sera at dilutions from 1:50 – 1:1000 in assay buffer added to the antigen-coated wells in duplicate. Serial dilutions of known concentrations of IgG were added to the F(ab)'2 IgG-coated wells in triplicate. Following incubation for 2 hours at room temperature, plates were washed with PBS-T and 25 µl alkaline phosphatase-conjugated goat anti-human IgG (Jackson ImmunoResearch) at a 1:1000 dilution in assay buffer added to each well and incubated for 1 hour at room temperature. Plates were then washed with PBS-T, and 25µl of alkaline phosphatase substrate (Sigma Aldrich) added. ODs were measured using a MultiskanFC

(Thermofisher) plate reader at 405nm and S1 & N-specific IgG titers interpolated from the IgG standard curve using 4PL regression curve-fitting on GraphPad Prism 8.

Pseudovirus production and neutralization assays

HIV-1 particles pseudotyped with SARS-Cov-2 spike were produced by seeding $3x10^6$ HEK-293T cells in 10ml complete DMEM (DMEM supplemented with 10% FBS, L-Glutamine, 100 IU/ml penicillin and 100 µg/ml streptomycin) in a T-75 culture flask. The following day cells were transfected with 9.1 µg of HIV p8.91 packaging plasmid [83] , 9.1 µg of HIV-1 luciferase reporter vector plasmid [28], 1.4 µg of WT-SARS-CoV-2 spike plasmid (2) and 60 µg of PEI-Max (Polysciences). Supernatants were harvested 48h later, filtered through a 0.45 µm filter and stored at -80°C. Neutralization assays were performed on 96-well plates by incubating serial dilutions of patient serum with pseudovirus for 1h at 37°C 5% CO_2. HeLa ACE-2 cells (gift from James E Voss, Scripps Institute) were then added to the assay (10,000 cells per 100 µL per well). After 48/72h at 37°C 5% CO_2, supernatants were removed, and the cells were lysed; Brightglo luciferase substrate (Promega) was added to the plates and RLU read on a Glomax luminometer (Promega) as a proxy for infection. Measurements were performed in duplicate and fifty percent inhibitory dilution (ID50) values were calculated using GraphPad Prism 8.

IgG Purification

For individuals on ART, to avoid off-target neutralization due to the HIV pseudovirus backbone, we purified IgG from serum using Mini Bio-Spin Chromatography Columns (BioRad) by incubating sera with a resin of protein G Sepharose beads (GE Healthcare) for 2h, eluting with 0.1M Glycine (pH 2.2) into 2M Tris-base, concentrating the IgG-containing fraction in a 50kD

concentrator (Amicon, Merck) and quantifying the amount of IgG by Nanodrop. The purified IgG was serially diluted from 200 µg/ml in neutralization assays and the resulting ID50 calculated using the total IgG concentration of each serum sample prior to purification.

Standardized ELISA for measurement of CMV-specific IgG levels in plasma

The levels of CMV-specific IgG were measured using the Abcam Anti-Cytomegalovirus (CMV) IgG Human ELISA kit following manufacturer's instructions. Assays were run in duplicate and mean values per participant are reported in International Units (IU) per ml.

Phenotypic flow cytometric analysis

The fluorochrome-conjugated antibodies used in this study are listed in **Table. S2**. Briefly, purified cryopreserved PBMCs were thawed and rested for one hour at 37 °C in complete RPMI medium (RPMI supplemented with Penicillin-Streptomycin, L-Glutamine, HEPES, non-essential amino acids, 2-Mercaptoethanol, and 10% Fetal bovine serum (FBS)). Cells were then washed, resuspended in PBS, and surface stained at 4°C for 20 min with different combinations of antibodies in the presence of fixable live/dead stain (Invitrogen). Cells were then fixed and permeabilized for detection of intracellular antigens. The Foxp3 intranuclear staining buffer kit (eBioscience) was used according to the manufacturer's instructions for the detection of intranuclear markers. Samples were acquired on a BD Fortessa X20 using BD FACSDiva8.0 (BD Bioscience) and subsequent data analysis was performed using FlowJo 10 (TreeStar). Stochastic neighbor embedding (SNE) analysis was undertaken on the mrc.cytobank platform to enable visualization of high-dimensional data in two-dimensional representations, avoiding the bias that can be introduced by manual gating of specific subsets [84].

Peptide Pools:

For detection of virus-specific T cell responses, PBMCs were stimulated with the following peptide pools:

1. SARS-CoV-2 Spike: total of 15 to18-mers overlapping by 10 amino acid residues for Spike (S) synthesized using Two-dimensional peptide Matrix pools, divided into 16 "minipools" P1-P16 and grouped into pools S1 (P1-8) and S2 (P 9-16) [40].
2. SARS-CoV-2 Structural and accessory proteins: 15-mer peptides overlapping by 10 amino acid residues for Membrane protein (M) (Miltenyibiotec), Nucleocapsid (N) (Miltenyibiotec), Envelope (Env) protein and open reading frame (ORF) 3, 6, 7 (a kind gift from Tao Dong) [40]
3. Non-SARS-CoV-2 antigens: Peptide pools of the pp65 protein of human cytomegalovirus (CMV) (Miltenyibiotec, and NIH AIDS Reagent Repository), or HIVconsv peptide pools (NIH AIDS Reagent Repository) HIV-1 and Influenza HLA class I-restricted T cell epitope (ProImmune). CD8 T cell epitopes of human influenza, CMV and EBV viruses (namely FEC controls, NIH AIDS Reagent Repository) were used as positive controls.

Ex vivo IFN-γ ELISpot Assay

IFN-γ ELISpot assays were performed with cryopreserved isolated PBMCs as described previously [40]. Briefly, ELISPOT plates (S5EJ044I10; Merck Millipore, Darmstadt, Germany) pre-wetted with 30 µl of 70% ethanol for a maximum of 2 minutes, washed with sterile PBS and coated overnight at 4 °C with anti–IFN-γ antibody (10 µg/ml in PBS; clone 1-D1K; Mabtech, Nacka

573 Strand, Sweden). Prior to use, plates were washed with PBS and blocked with R10 (RPMI
574 supplemented with Penicillin-Streptomycin, L-Glutamine, and 10% FBS) for 1 hour at 37 °C. The
575 cells were plated at 2×10^5 cells/well for most of the participants or 1×10^5 cells/well for
576 participants with lower cell recovery. Cells were cultured with overlapping peptide pools at
577 2 μg/ml or PHA (Sigma Aldrich, St Louis, MO) at 10 μg/ml as a positive control for 16-18 hours
578 at 37 °C. Cells lacking peptide stimulation were used as a negative control. Plates were then
579 washed four times with 0.05% Tween/PBS (Sigma-Aldrich) followed by two washes with PBS
580 and then incubated for 2 hr at RT with biotinylated anti-IFN-γ (1 μg/mL; clone mAb-7B6-1;
581 Mabtech). After six further washes, cells were incubated with alkaline phosphatase-conjugated
582 streptavidin (Mabtech) at 1:1000 dilution for 1 hr at RT. Plates were then washed six times and
583 developed using VECTASTAIN® Elite ABC-HRP according to the manufacturer's instructions
584 (Mabtech). All assays were performed in duplicate. Spots were counted using an automated
585 ELISpot Reader System (Autoimmun Diagnostika GmbH). Results are reported as difference in
586 (Δ) spot forming units (SFU) per 10^6 PBMCs between the peptide-stimulated and negative control
587 conditions. Responses that were found to be lower than two standard deviations of the sample
588 specific control were excluded. An additional threshold was set at > 5 SFU/10^6 PBMCs, and results
589 were excluded if positive control wells (PHA, FEC) were negative.
590
591 **Intracellular cytokine stimulation (ICS) functional assay**
592 ICS was performed as described previously [85]. Briefly, purified PBMCs were thawed and rested
593 overnight at 37 °C and 5% carbon dioxide in complete RPMI medium. After overnight rest,
594 PBMCs were stimulated for 6 h with 2μg/mL of SARS-CoV-2 peptide pools, Influenza, HIV-1
595 Gag or cytomegalovirus (CMV)-pp65 peptide pools, or with 0.005% dimethyl sulphoxide

(DMSO) as a negative control in the presence of αCD28/αCD49d co-Stim antibodies (1 μg ml^{-1}) GolgiStop (containing Monensin, 2 μmol/L), GolgiPlug (containing brefeldin A, 10 μg ml^{-1}) (BD Biosciences) and anti-CD107α BV421 antibody (BD Biosciences). After stimulation, cells were washed and stained with anti-CCR7 (BioLegend) for 30 min at 37 °C and then surface stained at 4°C for 20 min with different combinations of surface antibodies in the presence of fixable live/dead stain (Invitrogen). Cells were then fixed and permeabilised (CytoFix/CytoPerm; BD Biosciences) followed by intracellular cytokine with IFN-γ APC, CD154 PE-Cy7 (BioLegend), TNF-α FITC (BD Biosciences) and PerCP-eFluor 710 IL-2 (eBioscience). Samples were acquired on a BD Fortessa X20 using BD FACSDiva8.0 (BD Bioscience) and data analysed using FlowJo 10 (TreeStar). The gates applied for the identification of virus-specific CD4 and CD8 T cells were based on the double-positive populations for interferon-γ (IFN-γ), Tumour necrosis factor (TNF-α), interleukin-2 (IL-2), and CD40 ligand (CD154). The total population of SARS-CoV-2 CD4 T cells was calculated by summing the magnitude of $CD154^{+}IFN\text{-}\gamma^{+}$, $CD154^{+}IL\text{-}2^{+}$, and $CD154^{+}$ $TNF\text{-}\alpha^{+}$ responses; SARS-CoV-2 CD8 T cells were defined as ($IFN\text{-}\gamma^{+}TNF\text{-}\alpha^{+}$, $IFN\text{-}\gamma^{+}IL\text{-}2^{+}$). Antibodies used in the ICS assay are listed in **Supplementary Table 2**.

Statistics:

Prism 8 (GraphPad Software) was used for statistical analysis as follows: the Mann–Whitney *U*-test was used for single comparisons of independent groups, the Wilcoxon-test paired *t*-test was used to compare two paired groups. The non-parametric Spearman test was used for correlation analysis. The statistical significances are indicated in the figures (*$p < 0.05$, **$p < 0.01$, ***$p < 0.001$, and ****$p < 0.0001$). Polyfunctionality tests were performed in SPICE version 6.0.

Acknowledgments: We are grateful to Rebecca Matthews, Thomas Fernandez, Nnenna Ngwu the clinical research teams at Mortimer Market Centre and Ian Charleson Day Centre and all the clinic staff and participants. We would like to thank Chloe Rees-Spear for technical assistance and James E. Voss for the kind gift of HeLa cells stably expressing ACE2.

Funding: This work was supported by MRC grant MR/M008614 and NIH R01AI55182 (DP) and by UCL Coronavirus Response Fund (LEM) made possible through generous donations from UCL's supporters, alumni and friends**.** LEM is supported by a Medical Research Council Career Development Award (MR/R008698/1). ET is supported by a Medical Research Council DTP studentship (MR/N013867/1). DHB is supported by a Wellcome Trust PhD studentship in the Genomics and Statistical medicine doctoral training programme in Oxford.

Author contributions: AA, EGM, ET performed experiments, acquisition of data, analysis and drafting of the manuscript; DHB, JK, BC, NFP, LM, AR, CR, CE performed experiments and contributed to acquisition of data and analysis; PC, PP, LW, FB, SK, TD, LD, SRJ contributed to study design, data interpretation and critical editing of the manuscript. LEM, DP: conception and design of study, data analysis and interpretation, critical revision of the manuscript and study supervision.

Competing interests: The authors have declared that no conflict of interest exists.

Data and materials availability: Data can be made available by request to the corresponding authors.

Figure Legends:

Fig.1: Antibody response in HIV positive and negative donors recovered from COVID-19 disease.

a Seropositivity screen of plasma samples for antibodies against the external Spike antigen, using a recombinant Spike $S1_{1-530}$ subunit protein (S1), and against the full-length internal Nucleoprotein (N) antigen to confirm prior infection in HIV negative and positive donors. A sample absorbance greater than 4-fold above the average background of the assay was regarded as positive. Black dots denote laboratory confirmed cases and grey dots suspected/household contacts. **b** Comparison of S1 IgG and N IgG antibody titers in HIV negative and **c** HIV positive donors. Red dots: hospitalized cases; Black dots: mild (non-hospitalized cases); blue dots: asymptomatic cases. **d** Correlation between S1 IgG and N IgG titers in HIV negative and positive donors. **e** Neutralization titers in HIV negative and positive donors. Dotted lines indicate detection limit, minimum ID50 and potent levels >1000. **f** Proportion of HIV negative and positive donors with neutralizing antibodies within the given ranges. **g** Correlation between S1 IgG titers and neutralization titers in HIV negative and positive donors. The non-parametric Spearman test was used for correlation analysis. *$p < 0.05$, **$p<0.01$

Fig.2: Similar SARS-CoV-2 specific T cell responses by IFN-γ-ELISpot in HIV positive and negative donors.

a Genome organization of SARS-CoV-2 **b** Dominance of the IFN-γ-ELISpot responses. Heatmap depicting the magnitude of the IFN-γ-ELISpot responses to the different SARS-CoV-2 peptide pools in HIV negative and HIV positive individuals. (n=30 in each group) **c** Magnitude of the IFN-γ-ELISpot responses. IFN-γ SFU/10^6 PBMCs are shown for SARS-CoV-2 Spike (S), Membrane (M) and Nucleocapsid (N) between HIV negative (green) and HIV positive (red). (n=30 per

group). **d** Magnitude of the IFN-γ-ELISpot responses for Total SARS-CoV-2 responses (S, M, N, ORF3a, ORF6, ORF7, ORF8 and Env), FEC and HIV Gag between HIV negative (green) and HIV positive (red). (n=30 per group). **e** Hierarchy of the IFNγ-ELISpot responses. IFN-γ SFU/10^6 PBMCs responses in order of magnitude within each group with the contribution of the responses to a specific pool shown by color legend. **f** Diversity of the IFN-γ-ELISpot responses. Number of pools each of the donors has shown positive responses in the IFN-γ-ELISpot assay. The total of SARS-CoV-2 pools tested was 7. **g** Proportion of T cell response magnitude in the HIV negative and HIV positive individuals. **h** Correlation between CD4:CD8 ratio in HIV infected individuals with their total SARS-CoV-2 responses, depicting disease severity per each donor (Red dots: hospitalized cases; Black dots: non-hospitalized cases; blue dots: asymptomatic cases.). The non-parametric Spearman test was used for correlation analysis. Two-way ANOVA was used for groups comparison. *$p < 0.05$, **$p<0.01$.

Fig.3: Interrelations between T cell and antibody responses in HIV positive and negative donors.

a Correlation of total SARS-CoV-2 responses with S1 IgG titers in HIV negative and **b** HIV positive. **c** Correlation of total SARS-CoV-2 responses with N IgG titers in HIV negative and **d** HIV positive subjects. Red dots: hospitalized cases; Black dots: non-hospitalized cases. **e** Hierarchy of the T cell responses ordered by the neutralizing capacity by their antibody titers for HIV negative and **f** HIV positive donors. The non-parametric Spearman test was used for correlation analysis. *$p < 0.05$, **$p<0.01$

Fig.4: Composition of SARS-CoV-2-specific T cells in convalescent HIV negative and HIV positive individuals.

Intracellular cytokine staining (ICS) was performed to detect cytokine-producing T cells to the indicated peptide pools in HIV negative (HIV-, n=12) and HIV positive individuals (HIV+, n=11). **a** Representative flow cytometric plots for the identification of antigen-specific CD4 T cells based on double expressions ($CD154^+IFN\text{-}\gamma^+$, $CD154^+IL\text{-}2^+$, and $CD154^+TNF\text{-}\alpha^+$) following 6-hour stimulation media alone (control) or overlapping SARS-CoV-2 peptides against Spike pool 1 and 2 (Spike), nucleoprotein (N), and membrane protein (M) directly *ex vivo*. **b** Frequency of aggregated CD4 T cell responses ($CD154^+IFN\text{-}\gamma^+$, $CD154^+IL\text{-}2^+$, and $CD154^+TNF\text{-}\alpha^+$) against Spike, M/N or combined (Spike and M/N) peptide pools. **c** Pie charts representing the relative proportions of Spike, M/N, or total (combined Spike and M/N) CD4 T cell responses for one (grey), two (green) or three (dark blue) cytokines, and pie arcs denoting IFN-γ, TNF-α and IL-2. **d** Representative flow cytometric plots for the identification of antigen-specific CD8 T cells based on the expression of ($IFN\text{-}\gamma^+$, $TNF\text{-}\alpha^+$, and $IL\text{-}2^+$) against the specified peptide pools or media alone (control). **e** Proportion of aggregated CD8 T cell responses against Spike, M/N or combined (Spike and M/N) responses. **f** Pie charts representing the relative proportions of Spike, M/N and combined CD8 T cell responses for one (grey), two (green) or three (dark blue) cytokines, and pie arcs showing IFN-γ, TNF-α and IL-2. **g** Comparison of the frequencies of summed SARS-CoV-2-specific CD4 and CD8 T cell responses against Spike and M/N proteins. **h** Correlation between the frequency of total SARS-CoV-2 specific-CD4 T cells and overall T cell responses detected by IFN-γ ELISpot responses or **i** ID50 neutralization titer (log10) in HIV negative and HIV positive individuals. Error bars represent SEM. The non-parametric Spearman test was used for correlation analysis; p values for individual correlation analysis within groups, HIV- (green) or HIV+(red) or

combined correlation analysis (black) are presented. Significance determined by Mann-Whitney *U* test or Wilcoxon matched- pairs signed rank test, *p<0.05, **p<0.01, ***p < 0.001. SPICE (simplified presentation of incredibly complex evaluations) was used for polyfunctional analysis.

Fig.5: Phenotypic characterization of SARS-CoV-2-specific CD4 and CD8 T cells from convalescent HIV negative and HIV positive subjects.

a Representative flow plots and **b** pie charts representing proportion of antigen-specific CD4 T cell with a $CD45RA^-/CCR7^+$ central memory (CM), $CD45RA^+/CCR7^+$ naïve, $CD45RA^+/CCR7^-$ terminally differentiated effector memory (TEMRA) and $CD45RA^-/CCR7^-$ effector memory (EM) phenotype from HIV negative (HIV-, n=12) and HIV positive individuals (HIV+, n=11) against SARS-CoV-2 Spike, M, N, CMV pp65 and HIV gag. **c** Representative flow plots and **d** pie charts representing proportion of $CD45RA^-/CCR7^+$ central memory (CM), $CD45RA^+/CCR7^+$ naïve, $CD45RA^+/CCR7^-$ terminally differentiated effector memory (TEMRA) and $CD45RA^-/CCR7^-$ effector memory (EM) antigen-specific CD8 T cell subsets against SARS-CoV-2 Spike, M, N, CMV pp65 and HIV gag. **e** Representative flow plots from an HIV negative donor (HIV-) and an HIV positive donor (HIV+) showing expression of CD154 and IFN-γ production from PD1+ and PD1- SARS-CoV-2-specific CD4 T cells and paired analysis of responses in HIV negative (HIV-, n=12) and HIV positive (HIV+, n=11) individuals. **f** Correlation between frequency of ($PD\text{-}1^+CD154^+IFN\text{-}\gamma^+$ SARS-CoV-2-specific CD4 T cells and DPSO in both groups. Significance determined by Wilcoxon matched-pairs signed rank test, *p<0.05, **p<0.01, ***p < 0.001. The non-parametric Spearman test was used for correlation analysis; p values for individual correlation analysis within groups, HIV-, HIV+, or combined correlation analysis (black) are presented.

Fig.6: Immune profile relationships between convalescent HIV positive and negative individuals.

a viSNE analysis of CD3 T cells in HIV negative (top panel) and HIV positive donors (lower panel). Each point on the high-dimensional mapping represents an individual cell and colour intensity represents expression of selected markers. **b** Frequency of CD4 and CD8 T cells out of total lymphocytes in SARS-CoV-2 convalescent HIV negative (HIV-, n=26) and HIV positive individuals (HIV+, n=19) via traditional gating. **c** Summary data of the proportion of $CD45RA^-/CCR7^+$ central memory (CM), $CD45RA^+/CCR7^+$ naïve, $CD45RA^+/CCR7^-$ terminally differentiated effector memory (TEMRA) and $CD45RA^-/CCR7^-$ effector memory (EM) CD4 and CD8 T cell subsets it the study groups. **d** Correlation between CD4:CD8 ratio and frequency of naïve CD4 T cells in HIV-positive individuals. **e** Correlation between frequency of naïve CD4 T cells and total SARS-CoV-2 T cell responses, detected via ELISpot, in HIV positive individuals. **f** Correlation between frequency of naïve CD4 T cells and **g** naïve CD8 T cells and age in HIV negative individuals. **h** Correlation between frequency of naïve CD4 T cells and **i** naïve CD8 T cells age in HIV positive donors. Significance determined by Mann-Whitney test, *$p<0.05$, **$p<0.01$, ***$p < 0.001$. The non-parametric Spearman test was used for correlation analysis.

Supplementary Materials:

Supplementary Fig.1: Antigen binding screen and associations between humoral responses and cohort parameters

Supplementary Fig.2: Magnitude of T cell responses and associations with HIV parameters, age, gender and ethnicity

Supplementary Fig.3: Cytokine profile of SARS-CoV-2-, CMV- and Gag- specific T cells

Supplementary Fig.4: Association between T cell immunophenotyping and SARS-CoV-2 adaptive immune responses

Supplementary Table 1: Cohort demographics and clinical characteristics

Supplementary Table 2: Antibodies used for phenotypic analysis and virus-specific T cell characterization

Supplementary Fig.1: Antigen binding screen and associations between humoral responses and cohort parameters. a Antigen binding screen in pre-pandemic samples from n=16 HIV positive donors and **b** the whole cohort with convalescent COVID-19 disease. Dotted lines indicate negative, low positive and positive threshold for absorbance [450nm]. **c** Correlation between age and S1 IgG titer according to gender in HIV negative donors and HIV positive subjects. **d** Correlation between age and ID50 according to gender in HIV negative donors and HIV positive subjects and **e** between DPSO and ID50 in the two study groups. **f** S1 IgG titer and ID50 levels summary dot plots according to ethnicity in HIV positive and negative donors. The non-parametric Spearman test was used for correlation analysis. $*p < 0.05$

Supplementary Fig.2: Magnitude of T cell responses and associations with HIV parameters, age, gender and ethnicity. a Percentage of responders to each peptide pools **b** Magnitude of the INF-γ-ELISpot responses. IFN-γ SFU/10^6 PBMCs are shown for SARS-CoV-2 ORF3a, ORF6, ORF7, ORF8 and Env between HIV negative (green) and HIV positive (red). (n=30 per group). **c** Magnitude of the total SARS-CoV-2 responses analyzed in pre-pandemic samples, confirmed

SARS-CoV-2 and suspected cases with clinical definition but found to be SARS-CoV-2 seronegative on screening. In suspected cases, orange dots depict HIV negative and brown dots HIV positive donors. Correlation between CD4:CD8 ratio in HIV infected individuals with their **d** Nucleocapsid and **e** Membrane responses, depicting disease severity per donor. Correlation of total SARS-CoV-2 responses with age in **f** HIV negative and **g** HIV positive, depicting disease severity per donor. **h** Correlation of total SARS-CoV-2 responses with DPSO in HIV negative and **i** HIV positive, depicting disease severity per donor. **j** Magnitude of the total SARS-CoV-2 responses by ethnicity and **k** gender between HIV negative and HIV positive. The non-parametric Spearman test was used for correlation analysis. Two-way ANOVA was used for group comparison. *$p < 0.05$, **$p<0.01$.

Supplementary Fig.3: Cytokine profile of SARS-CoV-2-, CMV- and Gag- specific T cells

a Frequency of SARS-CoV-2-specific $CD154^+$ CD4 T cells identified by expression of IFN-γ^+, IL-2^+, or TNF-α^+ or overall responses with at least one of the three cytokines (IFN-γ, TNF- α and IL-2) against Spike (S1 and S2 pools) **b** M/N or **c** combined (Spike and M/N) responses in HIV-negative (HIV-, n=12) and HIV positive individuals (HIV+, n=11) recovering from COVID-19 disease. **d** Representative flow plots and summary data **e** showing frequencies of overall ($CD154^+$IFN-γ^+, $CD154^+$IL-2^+, or $CD154^+$TNF-α^+) SARS-CoV-2-, CMV-, or Gag-specific CD4 T cell responses in the study groups. **f** Frequency of SARS-CoV-2-specific CD8 T cells identified by expression of IFN-γ^+, IL-2^+ or TNF-α^+, or overall responses with at least one of the three cytokines (IFN-γ, TNF- α and IL-2) against Spike (S1 and S2 pools) **g** M/N or **h** combined (Spike and M/N) responses in HIV-negative (HIV-, n=12) and HIV-seropositive individuals (HIV+, n=11). **i** Representative flow plots and **j** summary data showing frequencies of overall (IFN-γ^+, IL-2^+, or

800 TNF-α^+) SARS-CoV-2-, CMV-, or Gag-specific CD8 T cell responses in the study groups. Error
801 bars represent SEM. The non-parametric Spearman test was used for correlation analysis; p values
802 for individual correlation analysis within groups, HIV- (green) or HIV+ (red) or combined
803 correlation analysis (black) are presented. Significance determined by Mann-Whitney *U* test or
804 Wilcoxon matched- pairs signed rank test, *p<0.05, **p<0.01, ***p < 0.001.
805

806 **Supplementary Fig.4: Association between T cell immunophenotyping and SARS-CoV-2**
807 **adaptive immune responses**
808 **a** Representative flow plots and **b** summary data of the frequency of $CD38^+$ $HLADR^+$ CD4 and
809 CD8 T cells, and correlations between percentage of $CD38^+$ $HLADR^+$ CD4 and CD8 T cells and
810 total SARS-CoV-2-specific T cell responses in HIV-seronegative (HIV-, n=26) and HIV positive
811 individuals (HIV+, n=19). **c** Representative flow plots and **d** summary data of frequency of $PD\text{-}1^+$
812 $TIGIT^+$ CD4 and CD8 T cells, and correlations between percentage of $PD\text{-}1^+$ $TIGIT^+$ CD4 and
813 CD8 T cells and total SARS-CoV-2-specific T cell responses. **e** Representative flow plots showing
814 the gating strategy used to define total circulating and activated Tfh subsets in the study groups
815 and summary data. **f** Correlations between percentage of activated Tfh and S1 IgG or N IgG titers.
816 Significance determined by Mann-Whitney test, *p<0.05, **p<0.01, ***p < 0.001. The non-
817 parametric Spearman test was used for correlation analysis; combined correlation analysis is
818 depicted.
819
820

821 **References:**

822 1 Guan, W. J. *et al.* Clinical Characteristics of Coronavirus Disease 2019 in China. *The New*
823 *England journal of medicine* **382**, 1708-1720, doi:10.1056/NEJMoa2002032 (2020).

824 2 Harris, T. G., Rabkin, M. & El-Sadr, W. M. Achieving the fourth 90: healthy aging for
825 people living with HIV. *AIDS* **32**, 1563-1569, doi:10.1097/QAD.0000000000001870
826 (2018).

827 3 Williamson, E. J. *et al.* Factors associated with COVID-19-related death using
828 OpenSAFELY. *Nature* **584**, 430-436, doi:10.1038/s41586-020-2521-4 (2020).

829 4 Wu, Z. & McGoogan, J. M. Characteristics of and Important Lessons From the
830 Coronavirus Disease 2019 (COVID-19) Outbreak in China: Summary of a Report of 72314
831 Cases From the Chinese Center for Disease Control and Prevention. *JAMA* **323**, 1239-
832 1242, doi:10.1001/jama.2020.2648 (2020).

833 5 Guaraldi, G. *et al.* Premature age-related comorbidities among HIV-infected persons
834 compared with the general population. *Clinical infectious diseases : an official publication*
835 *of the Infectious Diseases Society of America* **53**, 1120-1126, doi:10.1093/cid/cir627
836 (2011).

837 6 De Francesco, D. *et al.* Do people living with HIV experience greater age advancement
838 than their HIV-negative counterparts? *AIDS* **33**, 259-268,
839 doi:10.1097/QAD.0000000000002063 (2019).

840 7 Deeks, S. G. & Phillips, A. N. HIV infection, antiretroviral treatment, ageing, and non-
841 AIDS related morbidity. *BMJ* **338**, a3172, doi:10.1136/bmj.a3172 (2009).

842 8 Moir, S. & Fauci, A. S. B-cell responses to HIV infection. *Immunological reviews* **275**, 33-
843 48, doi:10.1111/imr.12502 (2017).

9 Pallikkuth, S. *et al.* Impaired peripheral blood T-follicular helper cell function in HIV-infected nonresponders to the 2009 H1N1/09 vaccine. *Blood* **120**, 985-993, doi:10.1182/blood-2011-12-396648 (2012).

10 Blanco, J. L. *et al.* COVID-19 in patients with HIV: clinical case series. *Lancet HIV* **7**, e314-e316, doi:10.1016/S2352-3018(20)30111-9 (2020).

11 Cooper, T. J., Woodward, B. L., Alom, S. & Harky, A. Coronavirus disease 2019 (COVID-19) outcomes in HIV/AIDS patients: a systematic review. *HIV medicine* **21**, 567-577, doi:10.1111/hiv.12911 (2020).

12 Inciarte, A. *et al.* Clinical characteristics, risk factors, and incidence of symptomatic coronavirus disease 2019 in a large cohort of adults living with HIV: a single-center, prospective observational study. *AIDS* **34**, 1775-1780, doi:10.1097/QAD.0000000000002643 (2020).

13 Sigel, K. *et al.* Coronavirus 2019 and People Living With Human Immunodeficiency Virus: Outcomes for Hospitalized Patients in New York City. *Clinical infectious diseases : an official publication of the Infectious Diseases Society of America* **71**, 2933-2938, doi:10.1093/cid/ciaa880 (2020).

14 Geretti, A. M. *et al.* Outcomes of COVID-19 related hospitalization among people with HIV in the ISARIC WHO Clinical Characterization Protocol (UK): a prospective observational study. *Clinical infectious diseases : an official publication of the Infectious Diseases Society of America*, doi:10.1093/cid/ciaa1605 (2020).

15 Bhaskaran, K. *et al.* HIV infection and COVID-19 death: a population-based cohort analysis of UK primary care data and linked national death registrations within the

OpenSAFELY platform. *Lancet HIV* **8**, e24-e32, doi:10.1016/S2352-3018(20)30305-2 (2021).

16 Boulle, A. *et al.* Risk factors for COVID-19 death in a population cohort study from the Western Cape Province, South Africa. *Clinical infectious diseases : an official publication of the Infectious Diseases Society of America*, doi:10.1093/cid/ciaa1198 (2020).

17 Hoffmann, C. *et al.* Immune deficiency is a risk factor for severe COVID-19 in people living with HIV. *HIV medicine*, doi:10.1111/hiv.13037 (2020).

18 Rydyznski Moderbacher, C. *et al.* Antigen-Specific Adaptive Immunity to SARS-CoV-2 in Acute COVID-19 and Associations with Age and Disease Severity. *Cell* **183**, 996-1012 e1019, doi:10.1016/j.cell.2020.09.038 (2020).

19 Oja, A. E. *et al.* Divergent SARS-CoV-2-specific T- and B-cell responses in severe but not mild COVID-19 patients. *European journal of immunology* **50**, 1998-2012, doi:10.1002/eji.202048908 (2020).

20 Tan, A. T. *et al.* Early induction of functional SARS-CoV-2-specific T cells associates with rapid viral clearance and mild disease in COVID-19 patients. *Cell reports* **34**, 108728, doi:10.1016/j.celrep.2021.108728 (2021).

21 Crotty, S. A brief history of T cell help to B cells. *Nature reviews. Immunology* **15**, 185-189, doi:10.1038/nri3803 (2015).

22 Laidlaw, B. J., Craft, J. E. & Kaech, S. M. The multifaceted role of CD4(+) T cells in CD8(+) T cell memory. *Nature reviews. Immunology* **16**, 102-111, doi:10.1038/nri.2015.10 (2016).

23 Annika Fendler, L. A., Laura Amanda Boos, Fiona Byrne, Scott T.C. Shepherd, Ben Shum, Camille L. Gerard, Barry Ward, Wenyi Xie, Maddalena Cerrone, Georgina H. Cornish,

Martin Pule, Leila Mekkaoui, Kevin W. Ng, Richard Stone, Camila Gomes, Helen R. Flynn, Ana Agua-Doce, Phillip Hobson, Simon Caidan, Mike Howell, Robert Goldstone, Mike Gavrielides, Emma Nye, Bram Snijders, James Macrae, Jerome Nicod, Adrian Hayday, Firza Gronthoud, Christina Messiou, David Cunningham, Ian Chau, Naureen Starling, Nicholas Turner, Jennifer Rusby, Liam Welsh, Nicholas van As, Robin Jones, Joanne Droney, Susana Banerjee, Kate Tatham, Shaman Jhanji, Mary O'Brien, Olivia Curtis, Kevin Harrington, Shreerang Bhide, Tim Slattery, Yasir Khan, Zayd Tippu, Isla Leslie, Spyridon Gennatas, Alicia Okines, Alison Reid, Kate Young, Andrew Furness, Lisa Pickering, Sonia Ghandi, Steve Gamblin, Charles Swanton, Emma Nicholson, Sacheen Kumar, Nadia Yousaf, Katalin Wilkinson, Anthony Swerdlow, Ruth Harvey, George Kassiotis, Robert Wilkinson, James Larkin, Samra Turajlic. Adaptive immunity to SARS-CoV-2 in cancer patients: The CAPTURE study. *medRxiv 2020.12.21.20248608*, doi:doi: https://doi.org/10.1101/2020.12.21.20248608 (2020).

24 Calvet, J. *et al.* CD4 and CD8 Lymphocyte Counts as Surrogate Early Markers for Progression in SARS-CoV-2 Pneumonia: A Prospective Study. *Viruses* **12**, doi:10.3390/v12111277 (2020).

25 Dan, J. M. *et al.* Immunological memory to SARS-CoV-2 assessed for up to eight months after infection. *bioRxiv*, doi:10.1101/2020.11.15.383323 (2020).

26 Ripperger, T. J. *et al.* Orthogonal SARS-CoV-2 Serological Assays Enable Surveillance of Low-Prevalence Communities and Reveal Durable Humoral Immunity. *Immunity* **53**, 925-933 e924, doi:10.1016/j.immuni.2020.10.004 (2020).

27 Wajnberg, A. *et al.* Robust neutralizing antibodies to SARS-CoV-2 infection persist for months. *Science* **370**, 1227-1230, doi:10.1126/science.abd7728 (2020).

912 28 Seow, J. *et al.* Longitudinal observation and decline of neutralizing antibody responses in
913 the three months following SARS-CoV-2 infection in humans. *Nat Microbiol* **5**, 1598-
914 1607, doi:10.1038/s41564-020-00813-8 (2020).
915 29 Robbiani, D. F. *et al.* Convergent antibody responses to SARS-CoV-2 in convalescent
916 individuals. *Nature* **584**, 437-442, doi:10.1038/s41586-020-2456-9 (2020).
917 30 Reynolds, C. J. *et al.* Discordant neutralizing antibody and T cell responses in
918 asymptomatic and mild SARS-CoV-2 infection. *Science immunology* **5**,
919 doi:10.1126/sciimmunol.abf3698 (2020).
920 31 Sekine, T. *et al.* Robust T Cell Immunity in Convalescent Individuals with Asymptomatic
921 or Mild COVID-19. *Cell* **183**, 158-168 e114, doi:10.1016/j.cell.2020.08.017 (2020).
922 32 Le Bert, N. *et al.* SARS-CoV-2-specific T cell immunity in cases of COVID-19 and SARS,
923 and uninfected controls. *Nature* **584**, 457-462, doi:10.1038/s41586-020-2550-z (2020).
924 33 Ng, K. W. *et al.* Preexisting and de novo humoral immunity to SARS-CoV-2 in humans.
925 *Science* **370**, 1339-1343, doi:10.1126/science.abe1107 (2020).
926 34 Sattler, A. *et al.* SARS-CoV-2-specific T cell responses and correlations with COVID-19
927 patient predisposition. *The Journal of clinical investigation* **130**, 6477-6489,
928 doi:10.1172/JCI140965 (2020).
929 35 George, V. K. *et al.* HIV infection Worsens Age-Associated Defects in Antibody
930 Responses to Influenza Vaccine. *The Journal of infectious diseases* **211**, 1959-1968,
931 doi:10.1093/infdis/jiu840 (2015).
932 36 Wang, M., Luo, L., Bu, H. & Xia, H. One case of coronavirus disease 2019 (COVID-19)
933 in a patient co-infected by HIV with a low CD4(+) T-cell count. *Int J Infect Dis* **96**, 148-
934 150, doi:10.1016/j.ijid.2020.04.060 (2020).

37 O'Nions, J. *et al.* SARS-CoV-2 antibody responses in patients with acute leukaemia. *Leukemia* **35**, 289-292, doi:10.1038/s41375-020-01103-2 (2021).

38 Pickering, S. *et al.* Comparative assessment of multiple COVID-19 serological technologies supports continued evaluation of point-of-care lateral flow assays in hospital and community healthcare settings. *PLoS pathogens* **16**, e1008817, doi:10.1371/journal.ppat.1008817 (2020).

39 Grifoni, A. *et al.* Targets of T Cell Responses to SARS-CoV-2 Coronavirus in Humans with COVID-19 Disease and Unexposed Individuals. *Cell* **181**, 1489-1501 e1415, doi:10.1016/j.cell.2020.05.015 (2020).

40 Peng, Y. *et al.* Broad and strong memory CD4(+) and CD8(+) T cells induced by SARS-CoV-2 in UK convalescent individuals following COVID-19. *Nature immunology* **21**, 1336-1345, doi:10.1038/s41590-020-0782-6 (2020).

41 Braun, J. *et al.* SARS-CoV-2-reactive T cells in healthy donors and patients with COVID-19. *Nature* **587**, 270-274, doi:10.1038/s41586-020-2598-9 (2020).

42 Owen, R. E. *et al.* Loss of T cell responses following long-term cryopreservation. *Journal of immunological methods* **326**, 93-115, doi:10.1016/j.jim.2007.07.012 (2007).

43 Breton, G. *et al.* Persistent Cellular Immunity to SARS-CoV-2 Infection. *bioRxiv*, doi:10.1101/2020.12.08.416636 (2020).

44 De Biasi, S. *et al.* Marked T cell activation, senescence, exhaustion and skewing towards TH17 in patients with COVID-19 pneumonia. *Nature communications* **11**, 3434, doi:10.1038/s41467-020-17292-4 (2020).

45 Zheng, M. *et al.* Functional exhaustion of antiviral lymphocytes in COVID-19 patients. *Cell Mol Immunol* **17**, 533-535, doi:10.1038/s41423-020-0402-2 (2020).

46 Song, J. W. *et al.* Immunological and inflammatory profiles in mild and severe cases of COVID-19. *Nature communications* **11**, 3410, doi:10.1038/s41467-020-17240-2 (2020).

47 Rha, M. S. *et al.* PD-1-Expressing SARS-CoV-2-Specific CD8(+) T Cells Are Not Exhausted, but Functional in Patients with COVID-19. *Immunity* **54**, 44-52 e43, doi:10.1016/j.immuni.2020.12.002 (2021).

48 Chen, Z. & John Wherry, E. T cell responses in patients with COVID-19. *Nature reviews. Immunology* **20**, 529-536, doi:10.1038/s41577-020-0402-6 (2020).

49 Mathew, D. *et al.* Deep immune profiling of COVID-19 patients reveals distinct immunotypes with therapeutic implications. *Science* **369**, doi:10.1126/science.abc8511 (2020).

50 Roederer, M. *et al.* CD8 naive T cell counts decrease progressively in HIV-infected adults. *The Journal of clinical investigation* **95**, 2061-2066, doi:10.1172/JCI117892 (1995).

51 Douek, D. C. *et al.* Changes in thymic function with age and during the treatment of HIV infection. *Nature* **396**, 690-695, doi:10.1038/25374 (1998).

52 Breton, G. *et al.* Programmed death-1 is a marker for abnormal distribution of naive/memory T cell subsets in HIV-1 infection. *J Immunol* **191**, 2194-2204, doi:10.4049/jimmunol.1200646 (2013).

53 El-Far, M. *et al.* T-cell exhaustion in HIV infection. *Current HIV/AIDS reports* **5**, 13-19, doi:10.1007/s11904-008-0003-7 (2008).

54 Rodda, L. B. *et al.* Functional SARS-CoV-2-Specific Immune Memory Persists after Mild COVID-19. *Cell* **184**, 169-183 e117, doi:10.1016/j.cell.2020.11.029 (2021).

55 Zhang, J. *et al.* Spike-specific circulating T follicular helper cell and cross-neutralizing antibody responses in COVID-19-convalescent individuals. *Nat Microbiol* **6**, 51-58, doi:10.1038/s41564-020-00824-5 (2021).

56 Pallikkuth, S., de Armas, L., Rinaldi, S. & Pahwa, S. T Follicular Helper Cells and B Cell Dysfunction in Aging and HIV-1 Infection. *Frontiers in immunology* **8**, 1380, doi:10.3389/fimmu.2017.01380 (2017).

57 Gaebler, C. *et al.* Evolution of Antibody Immunity to SARS-CoV-2. *bioRxiv*, doi:10.1101/2020.11.03.367391 (2020).

58 Yu, J. *et al.* DNA vaccine protection against SARS-CoV-2 in rhesus macaques. *Science* **369**, 806-811, doi:10.1126/science.abc6284 (2020).

59 Anderson, E. J. *et al.* Safety and Immunogenicity of SARS-CoV-2 mRNA-1273 Vaccine in Older Adults. *The New England journal of medicine* **383**, 2427-2438, doi:10.1056/NEJMoa2028436 (2020).

60 Folegatti, P. M. *et al.* Safety and immunogenicity of the ChAdOx1 nCoV-19 vaccine against SARS-CoV-2: a preliminary report of a phase 1/2, single-blind, randomised controlled trial. *Lancet* **396**, 467-478, doi:10.1016/S0140-6736(20)31604-4 (2020).

61 Polack, F. P. *et al.* Safety and Efficacy of the BNT162b2 mRNA Covid-19 Vaccine. *The New England journal of medicine* **383**, 2603-2615, doi:10.1056/NEJMoa2034577 (2020).

62 Lumley, S. F. *et al.* Antibody Status and Incidence of SARS-CoV-2 Infection in Health Care Workers. *The New England journal of medicine*, doi:10.1056/NEJMoa2034545 (2020).

63 V Hall, S. F., A Charlett, A Atti, EJM Monk, R Simmons, E Wellington, MJ Cole, A Saei, B Oguti, K Munro, S Wallace, PD Kirwan, M Shrotri, A Vusirikala, S Rokadiya, M Kall,

M Zambon, M Ramsay, T Brooks, SIREN Study Group, CS Brown, MA Chand, S Hopkins. Do antibody positive healthcare workers have lower SARS-CoV-2 infection rates than antibody negative healthcare workers? Large multi-centre prospective cohort study (the SIREN study), England: June to November 2020. *medRxiv 2021.01.13.21249642*, doi:https://doi.org/10.1101/2021.01.13.21249642 (2020).

64 Kim, D. S., Rowland-Jones, S. & Gea-Mallorqui, E. Will SARS-CoV-2 Infection Elicit Long-Lasting Protective or Sterilising Immunity? Implications for Vaccine Strategies (2020). *Frontiers in immunology* **11**, 571481, doi:10.3389/fimmu.2020.571481 (2020).

65 Altmann, D. M. & Boyton, R. J. SARS-CoV-2 T cell immunity: Specificity, function, durability, and role in protection. *Science immunology* **5**, doi:10.1126/sciimmunol.abd6160 (2020).

66 Tang, F. *et al.* Lack of peripheral memory B cell responses in recovered patients with severe acute respiratory syndrome: a six-year follow-up study. *J Immunol* **186**, 7264-7268, doi:10.4049/jimmunol.0903490 (2011).

67 Opportunistic Infections Project Team of the Collaboration of Observational, H. I. V. E. R. i. E. i. E. *et al.* CD4 cell count and the risk of AIDS or death in HIV-Infected adults on combination antiretroviral therapy with a suppressed viral load: a longitudinal cohort study from COHERE. *PLoS Med* **9**, e1001194, doi:10.1371/journal.pmed.1001194 (2012).

68 Appay, V. & Sauce, D. Immune activation and inflammation in HIV-1 infection: causes and consequences. *The Journal of pathology* **214**, 231-241, doi:10.1002/path.2276 (2008).

69 Serrano-Villar, S. *et al.* The CD4:CD8 ratio is associated with markers of age-associated disease in virally suppressed HIV-infected patients with immunological recovery. *HIV medicine* **15**, 40-49, doi:10.1111/hiv.12081 (2014).

70 Serrano-Villar, S. *et al.* HIV-infected individuals with low CD4/CD8 ratio despite effective antiretroviral therapy exhibit altered T cell subsets, heightened CD8+ T cell activation, and increased risk of non-AIDS morbidity and mortality. *PLoS pathogens* **10**, e1004078, doi:10.1371/journal.ppat.1004078 (2014).

71 Helleberg, M. *et al.* Course and Clinical Significance of CD8+ T-Cell Counts in a Large Cohort of HIV-Infected Individuals. *The Journal of infectious diseases* **211**, 1726-1734, doi:10.1093/infdis/jiu669 (2015).

72 Serrano-Villar, S. *et al.* Increased risk of serious non-AIDS-related events in HIV-infected subjects on antiretroviral therapy associated with a low CD4/CD8 ratio. *PloS one* **9**, e85798, doi:10.1371/journal.pone.0085798 (2014).

73 SA Kemp, D. C., R Datir, S Gayed, A Jahun, M Hosmillo, IATM Ferreira, C Rees-Spear, P Mlcochova, Ines Ushiro Lumb, David Roberts, Anita Chandra, N Temperton, The CITIID-NIHR BioResource COVID-19 Collaboration, The COVID-19 Genomics UK (COG-UK) Consortium, K Sharrocks, E Blane, JAG Briggs, MJ van Gils, KGC Smith, JR Bradley, C Smith, RA Goldstein, IG Goodfellow, A Smielewska, JP Skittrall, T Gouliouris, E Gkrania-Klotsas, CJR Illingworth, LE McCoy, RK Gupta. Neutralising antibodies drive Spike mediated SARS-CoV-2 evasion. *medRxiv 2020.12.05.20241927*, doi:https://doi.org/10.1101/2020.12.05.20241927 (2020).

74 Houriiyah Tegally, E. W., Marta Giovanetti, Arash Iranzadeh, Vagner Fonseca, Jennifer Giandhari, Deelan Doolabh, Sureshnee Pillay, Emmanuel James San, Nokukhanya Msomi, Koleka Mlisana, Anne von Gottberg, Sibongile Walaza, Mushal Allam, Arshad Ismail, Thabo Mohale, Allison J Glass, Susan Engelbrecht, Gert Van Zyl, Wolfgang Preiser, Francesco Petruccione, Alex Sigal, Diana Hardie, Gert Marais, Marvin Hsiao, Stephen

Korsman, Mary-Ann Davies, Lynn Tyers, Innocent Mudau, Denis York, Caroline Maslo, Dominique Goedhals, Shareef Abrahams, Oluwakemi Laguda-Akingba, Arghavan Alisoltani-Dehkordi, Adam Godzik, Constantinos Kurt Wibmer, Bryan Trevor Sewell, José Lourenço, Luiz Carlos Junior Alcantara, Sergei L Kosakovsky Pond, Steven Weaver, Darren Martin, Richard J Lessells, Jinal N Bhiman, Carolyn Williamson, Tulio de Oliveira. Emergence and rapid spread of a new severe acute respiratory syndrome-related coronavirus 2 (SARS-CoV-2) lineage with multiple spike mutations in South Africa. *medRxiv 2020.12.21.20248640*, doi:https://doi.org/10.1101/2020.12.21.20248640 (2020).

75 Zuo J, D. A., Pearce H, et al. Robust SARS-CoV-2-specific T-cell immunity is maintained at 6 months following primary infection. *BioRxiv 2020.11.01.362319v1. www.biorxiv.org/content/10.1101/2020.11.01.362319v1* (2020).

76 Zimmerli, S. C. *et al.* HIV-1-specific IFN-gamma/IL-2-secreting CD8 T cells support CD4-independent proliferation of HIV-1-specific CD8 T cells. *Proceedings of the National Academy of Sciences of the United States of America* **102**, 7239-7244, doi:10.1073/pnas.0502393102 (2005).

77 Juno, J. A. *et al.* Humoral and circulating follicular helper T cell responses in recovered patients with COVID-19. *Nature medicine* **26**, 1428-1434, doi:10.1038/s41591-020-0995-0 (2020).

78 Boppana, S. *et al.* SARS-CoV-2-specific peripheral T follicular helper cells correlate with neutralizing antibodies and increase during convalescence. *medRxiv*, doi:10.1101/2020.10.07.20208488 (2020).

79 Zhou, R. *et al.* Acute SARS-CoV-2 Infection Impairs Dendritic Cell and T Cell Responses. *Immunity* **53**, 864-877 e865, doi:10.1016/j.immuni.2020.07.026 (2020).

80 Wibmer, C. K. *et al.* SARS-CoV-2 501Y.V2 escapes neutralization by South African COVID-19 donor plasma. *bioRxiv*, doi:10.1101/2021.01.18.427166 (2021).

81 Sandile Cele, I. G., Laurelle Jackson, Shi-Hsia Hwa, Houriiyah Tegally, Gila Lustig, Jennifer Giandhari, Sureshnee Pillay, Eduan Wilkinson, Yeshnee Naidoo, Farina Karim, Yashica Ganga, Khadija Khan, Alejandro B. Balazs, Bernadett I. Gosnell, Willem Hanekom, Mahomed-Yunus S. Moosa, NGS-SA, COMMIT-KZN Team, Richard J. Lessells, Tulio de Oliveira, Alex Sigal. Escape of SARS-CoV-2 501Y.V2 variants from neutralization by convalescent plasma. *medRxiv 2021.01.26.21250224*, doi:https://doi.org/10.1101/2021.01.26.21250224 (2021).

82 C Rees-Spear, L. M., SA Griffith, J Heaney, Y Aldon, JL Snitselaar, P Thomas, C Graham, J Seow, N Lee, A Rosa, C Roustan, CF Houlihan, RW Sanders, R Gupta, P Cherepanov, H Stauss, E Nastouli, KJ Doores, MJ van Gils, LE McCoy. The impact of Spike mutations on SARS-CoV-2 neutralization. *bioRxiv*, doi:https://doi.org/10.1101/2021.01.15.426849 (2021).

83 Zufferey, R., Nagy, D., Mandel, R. J., Naldini, L. & Trono, D. Multiply attenuated lentiviral vector achieves efficient gene delivery in vivo. *Nature biotechnology* **15**, 871-875, doi:10.1038/nbt0997-871 (1997).

84 Amir el, A. D. *et al.* viSNE enables visualization of high dimensional single-cell data and reveals phenotypic heterogeneity of leukemia. *Nature biotechnology* **31**, 545-552, doi:10.1038/nbt.2594 (2013).

85 Gupta, R. K. *et al.* HIV-1 remission following CCR5Delta32/Delta32 haematopoietic stem-cell transplantation. *Nature* **568**, 244-248, doi:10.1038/s41586-019-1027-4 (2019).

Figure 1

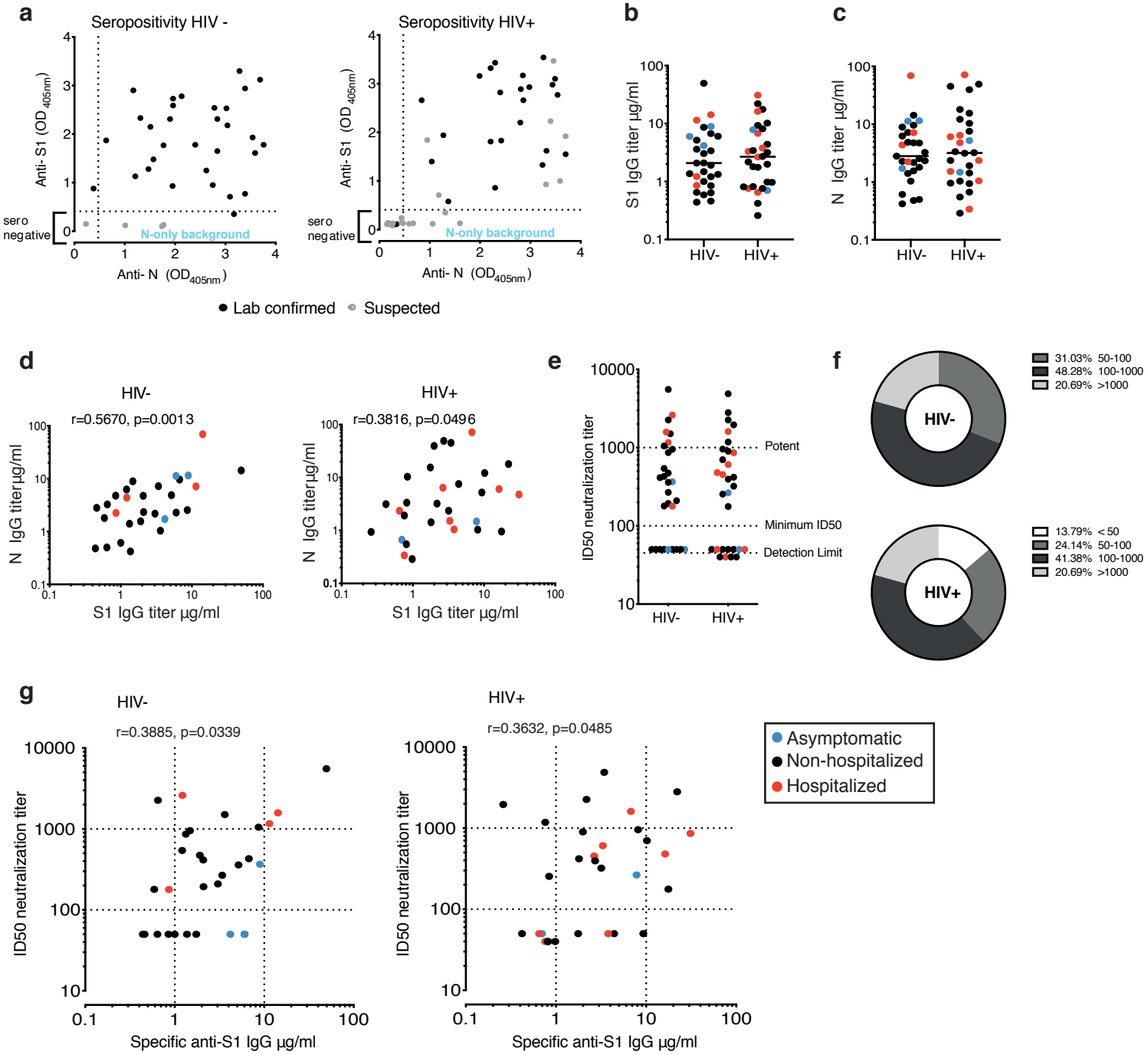
a
Seropositivity HIV -
Seropositivity HIV+
Anti- S1 (OD405nm)
Anti- N (OD405nm)
sero negative
N-only background
Lab confirmed
Suspected
b
S1 IgG titer µg/ml
HIV-
HIV+
c
N IgG titer µg/ml
d
HIV-
r=0.5670, p=0.0013
HIV+
r=0.3816, p=0.0496
N IgG titer µg/ml
S1 IgG titer µg/ml
e
ID50 neutralization titer
Potent
Minimum ID50
Detection Limit
f
HIV-
31.03% 50-100
48.28% 100-1000
20.69% >1000
HIV+
13.79% < 50
24.14% 50-100
41.38% 100-1000
20.69% >1000
g
HIV-
r=0.3885, p=0.0339
HIV+
r=0.3632, p=0.0485
ID50 neutralization titer
Specific anti-S1 IgG µg/ml
Asymptomatic
Non-hospitalized
Hospitalized

Figure 2

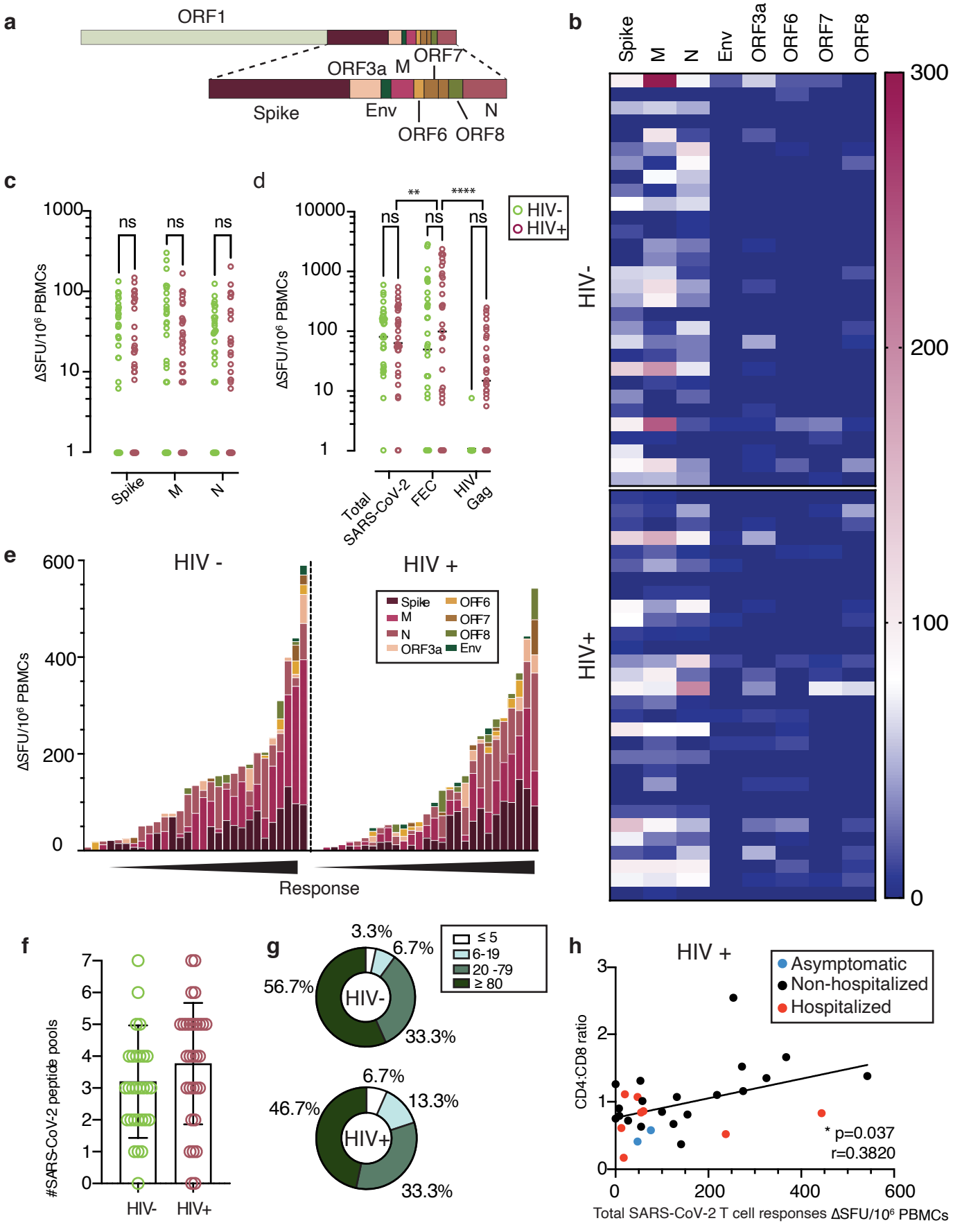
a
ORF1
ORF3a
M
ORF7
Spike
Env
N
ORF6
ORF8
b
Spike
M
N
Env
ORF3a
ORF6
ORF7
ORF8
HIV-
HIV+
300
200
100
0
c
ΔSFU/10⁶ PBMCs
1000
100
10
1
ns
ns
ns
Spike
M
N
d
ΔSFU/10⁶ PBMCs
10000
1000
100
10
1
**
****
ns
ns
ns
HIV-
HIV+
Total SARS-CoV-2
FEC
HIV Gag
e
HIV -
HIV +
ΔSFU/10⁶ PBMCs
600
400
200
0
Spike
M
N
ORF3a
ORF6
ORF7
ORF8
Env
Response
f
#SARS-CoV-2 peptide pools
7
6
5
4
3
2
1
0
HIV-
HIV+
g
3.3%
6.7%
56.7%
HIV-
33.3%
≤ 5
6-19
20 -79
≥ 80
6.7%
13.3%
46.7%
HIV+
33.3%
h
HIV +
Asymptomatic
Non-hospitalized
Hospitalized
CD4:CD8 ratio
3
2
1
0
* p=0.037
r=0.3820
0
200
400
600
Total SARS-CoV-2 T cell responses ΔSFU/10⁶ PBMCs

Figure 3

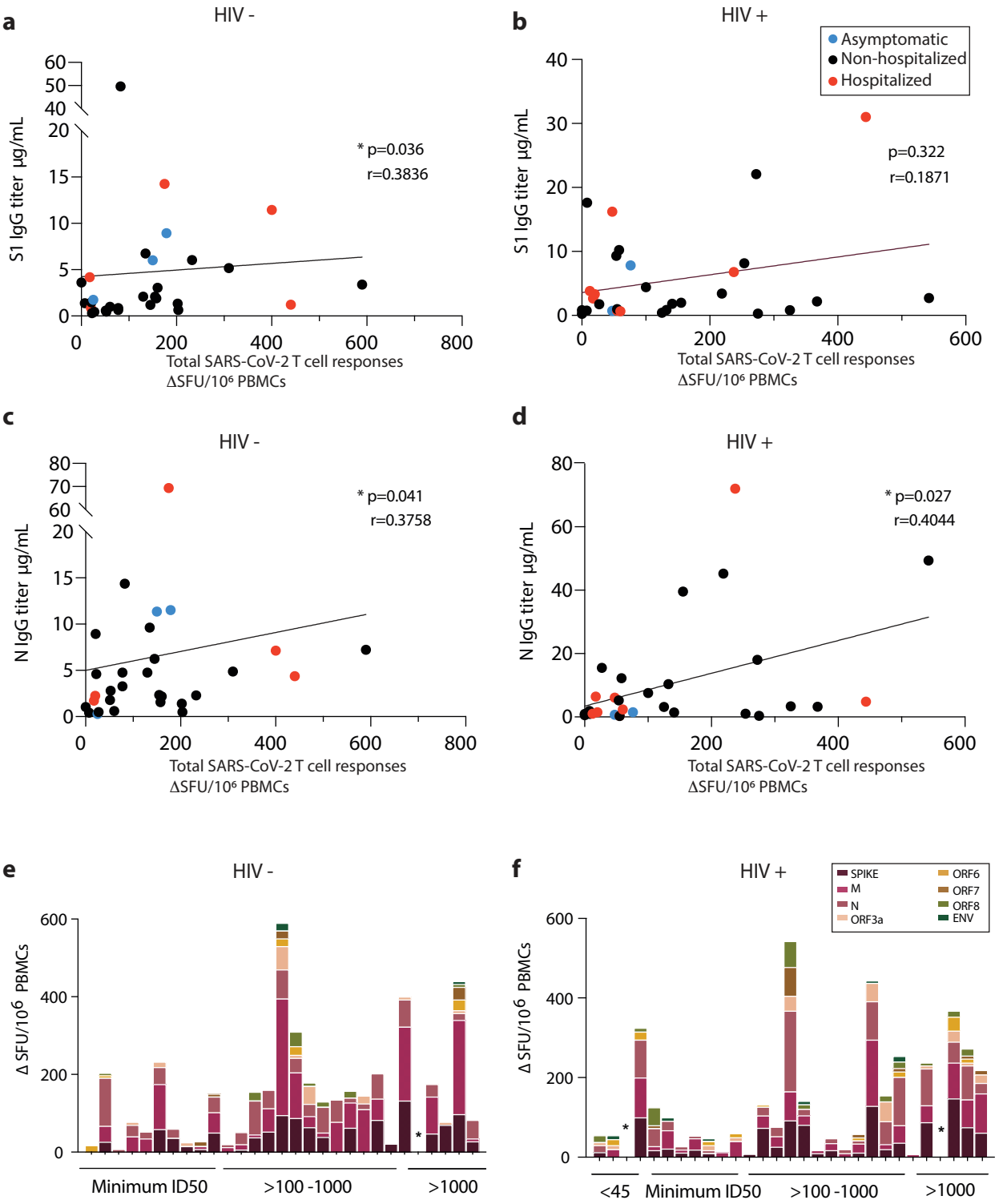
a
HIV -
S1 IgG titer µg/mL
* p=0.036
r=0.3836
Total SARS-CoV-2 T cell responses
ΔSFU/10⁶ PBMCs
b
HIV +
Asymptomatic
Non-hospitalized
Hospitalized
p=0.322
r=0.1871
c
HIV -
N IgG titer µg/mL
* p=0.041
r=0.3758
d
HIV +
* p=0.027
r=0.4044
e
HIV -
Δ SFU/10⁶ PBMCs
Minimum ID50
>100 -1000
>1000
f
HIV +
SPIKE
M
N
ORF3a
ORF6
ORF7
ORF8
ENV
<45
Minimum ID50
>100 -1000
>1000

Figure 4

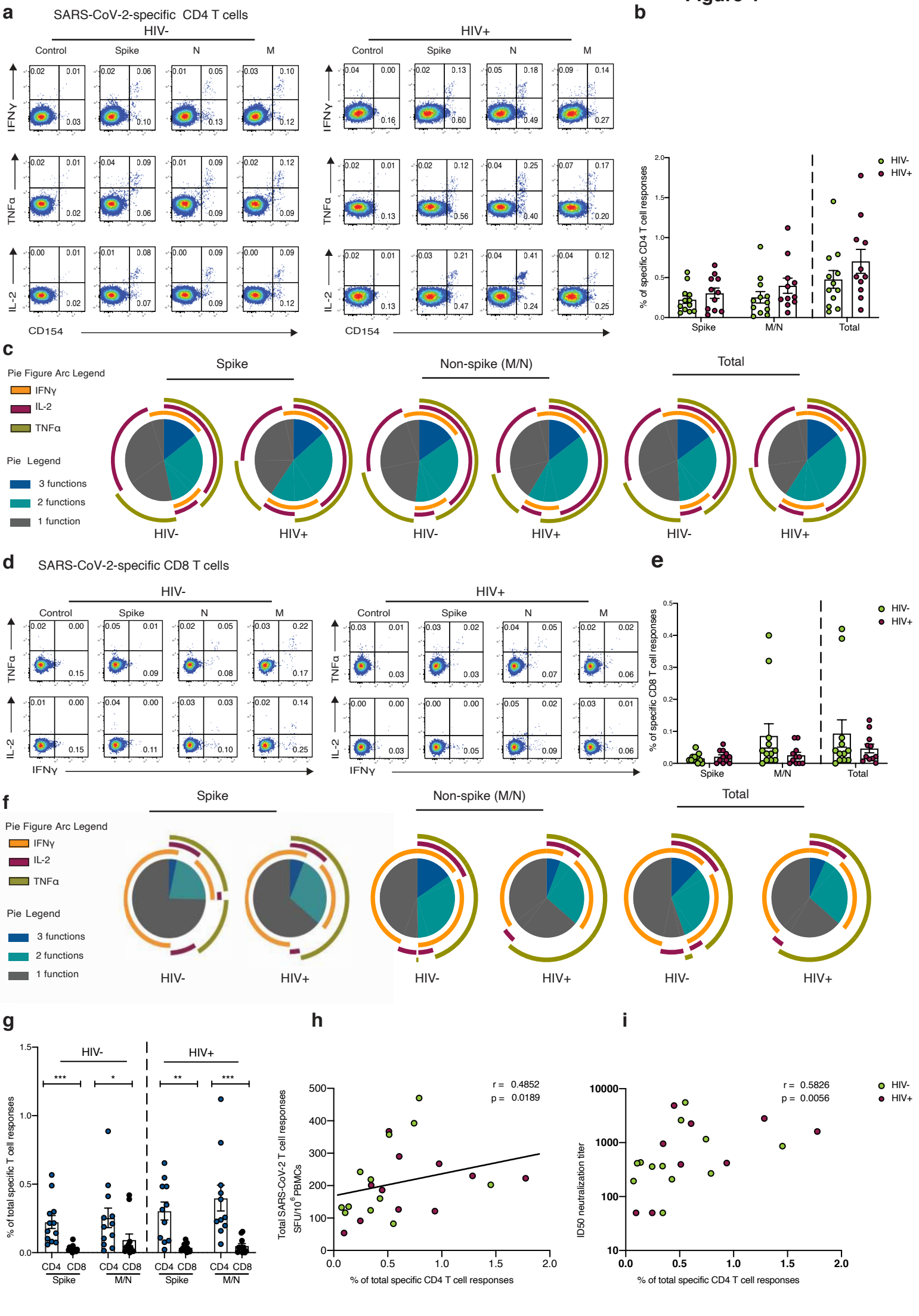
a
SARS-CoV-2-specific CD4 T cells
HIV-
HIV+
Control
Spike
N
M
IFNγ
TNFα
IL-2
CD154
b
% of specific CD4 T cell responses
HIV-
HIV+
Spike
M/N
Total
c
Pie Figure Arc Legend
IFNγ
IL-2
TNFα
Pie Legend
3 functions
2 functions
1 function
Spike
Non-spike (M/N)
Total
HIV-
HIV+
d
SARS-CoV-2-specific CD8 T cells
e
% of specific CD8 T cell responses
f
g
% of total specific T cell responses
CD4 CD8
h
Total SARS-CoV-2 T cell responses SFU/10^6 PBMCs
r = 0.4852
p = 0.0189
% of total specific CD4 T cell responses
i
ID50 neutralization titer
r = 0.5826
p = 0.0056

Figure 5

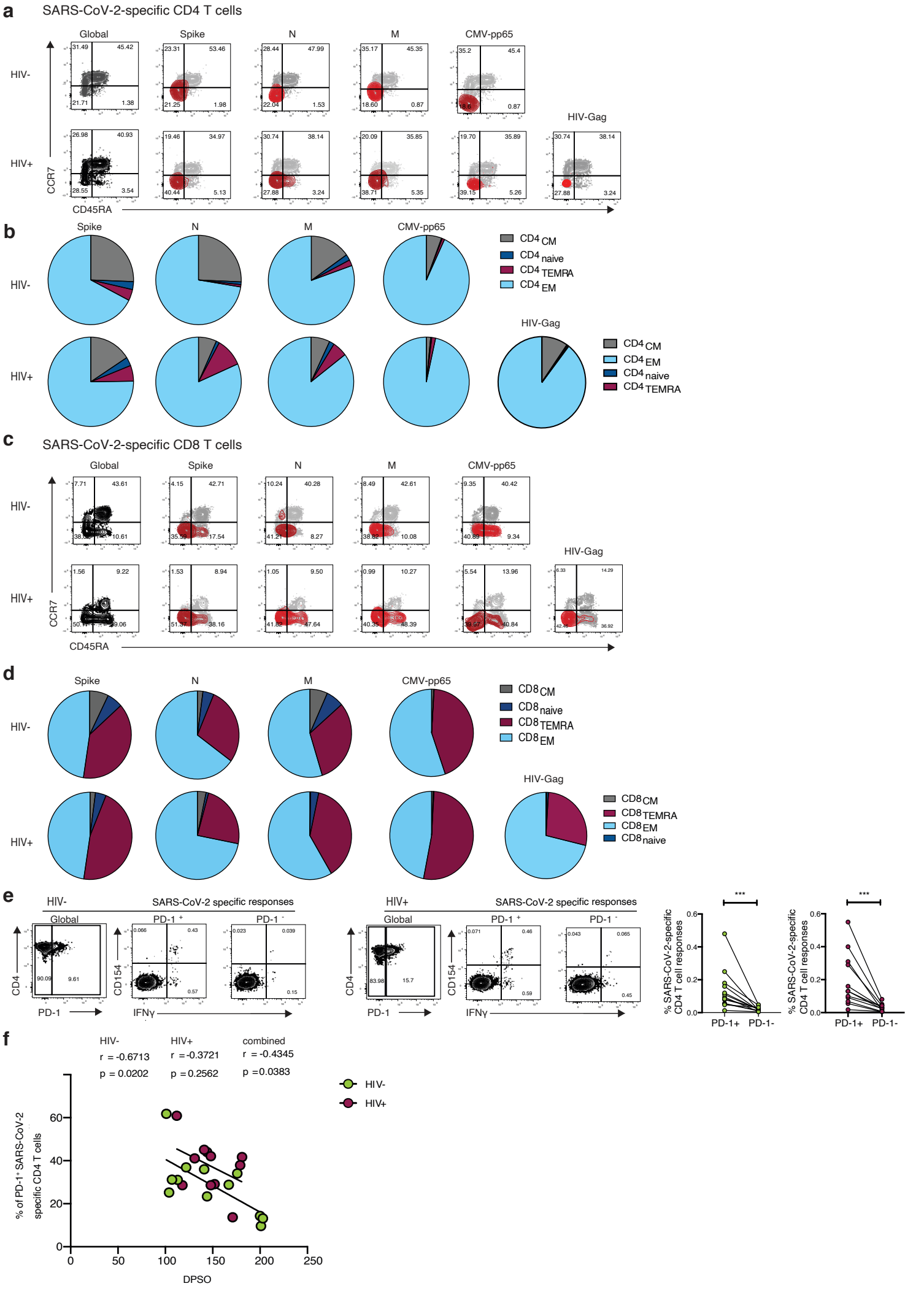
a
SARS-CoV-2-specific CD4 T cells
Global
Spike
N
M
CMV-pp65
HIV-Gag
HIV-
HIV+
CCR7
CD45RA
b
CD4 CM
CD4 naive
CD4 TEMRA
CD4 EM
c
SARS-CoV-2-specific CD8 T cells
d
CD8 CM
CD8 naive
CD8 TEMRA
CD8 EM
e
SARS-CoV-2 specific responses
PD-1 +
PD-1 -
CD4
PD-1
CD154
IFNγ
% SARS-CoV-2-specific CD4 T cell responses
PD-1+
PD-1-
f
HIV-
r = -0.6713
p = 0.0202
HIV+
r = -0.3721
p = 0.2562
combined
r = -0.4345
p = 0.0383
% of PD-1+ SARS-CoV-2 specific CD4 T cells
DPSO

Figure 6

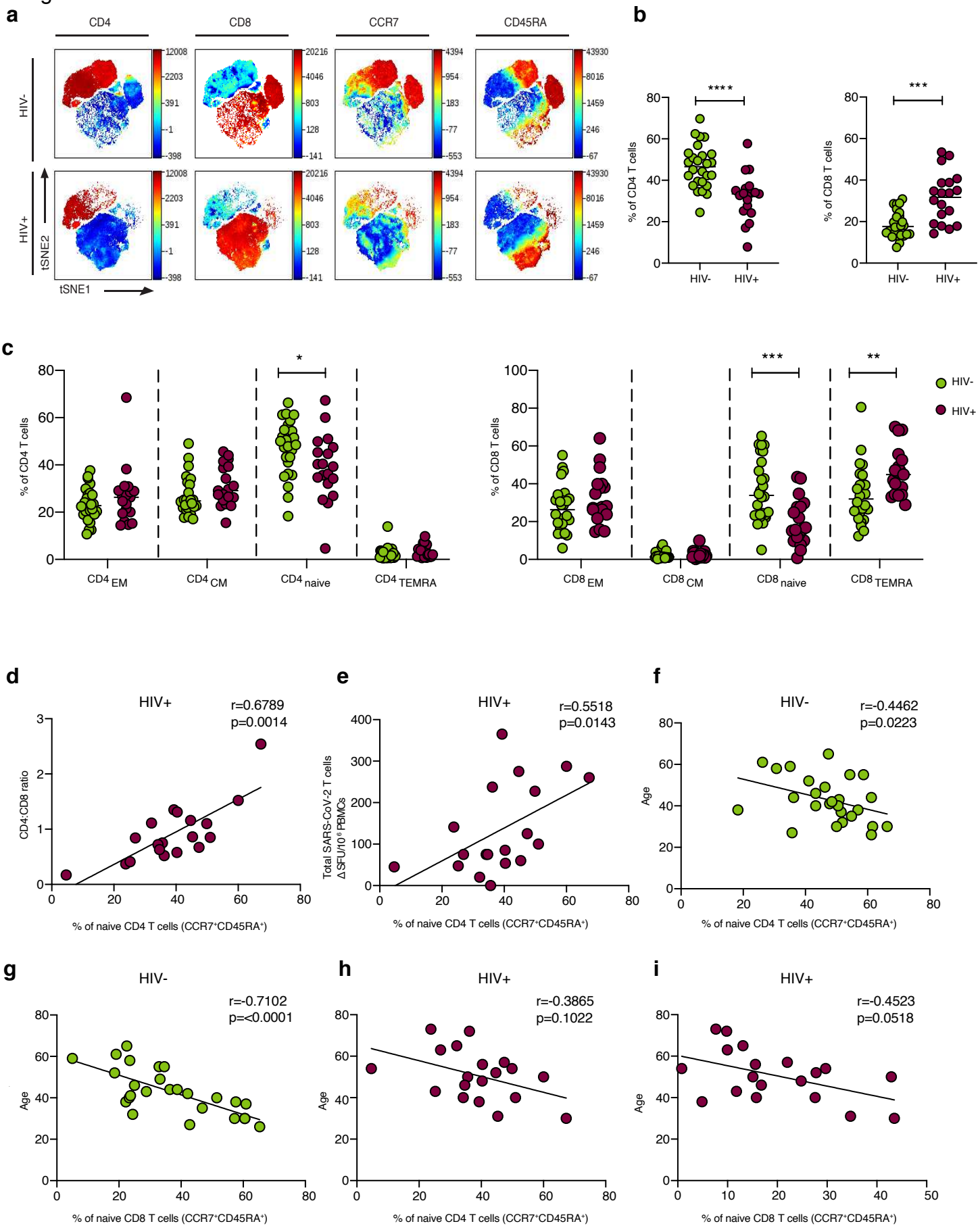
a
CD4
CD8
CCR7
CD45RA
HIV-
HIV+
tSNE2
tSNE1
12008
2203
391
-1
-398
20216
4046
803
128
-141
4394
954
183
-77
-553
43930
8016
1459
246
-67
b
****
***
% of CD4 T cells
% of CD8 T cells
HIV-
HIV+
c
*
***
**
% of CD4 T cells
% of CD8 T cells
CD4 EM
CD4 CM
CD4 naive
CD4 TEMRA
CD8 EM
CD8 CM
CD8 naive
CD8 TEMRA
HIV-
HIV+
d
HIV+
r=0.6789
p=0.0014
CD4:CD8 ratio
% of naive CD4 T cells (CCR7⁺CD45RA⁺)
e
HIV+
r=0.5518
p=0.0143
Total SARS-CoV-2 T cells
Δ SFU/10⁶ PBMCs
% of naive CD4 T cells (CCR7⁺CD45RA⁺)
f
HIV-
r=-0.4462
p=0.0223
Age
% of naive CD4 T cells (CCR7⁺CD45RA⁺)
g
HIV-
r=-0.7102
p=<0.0001
Age
% of naive CD8 T cells (CCR7⁺CD45RA⁺)
h
HIV+
r=-0.3865
p=0.1022
Age
% of naive CD4 T cells (CCR7⁺CD45RA⁺)
i
HIV+
r=-0.4523
p=0.0518
Age
% of naive CD8 T cells (CCR7⁺CD45RA⁺)

Figures

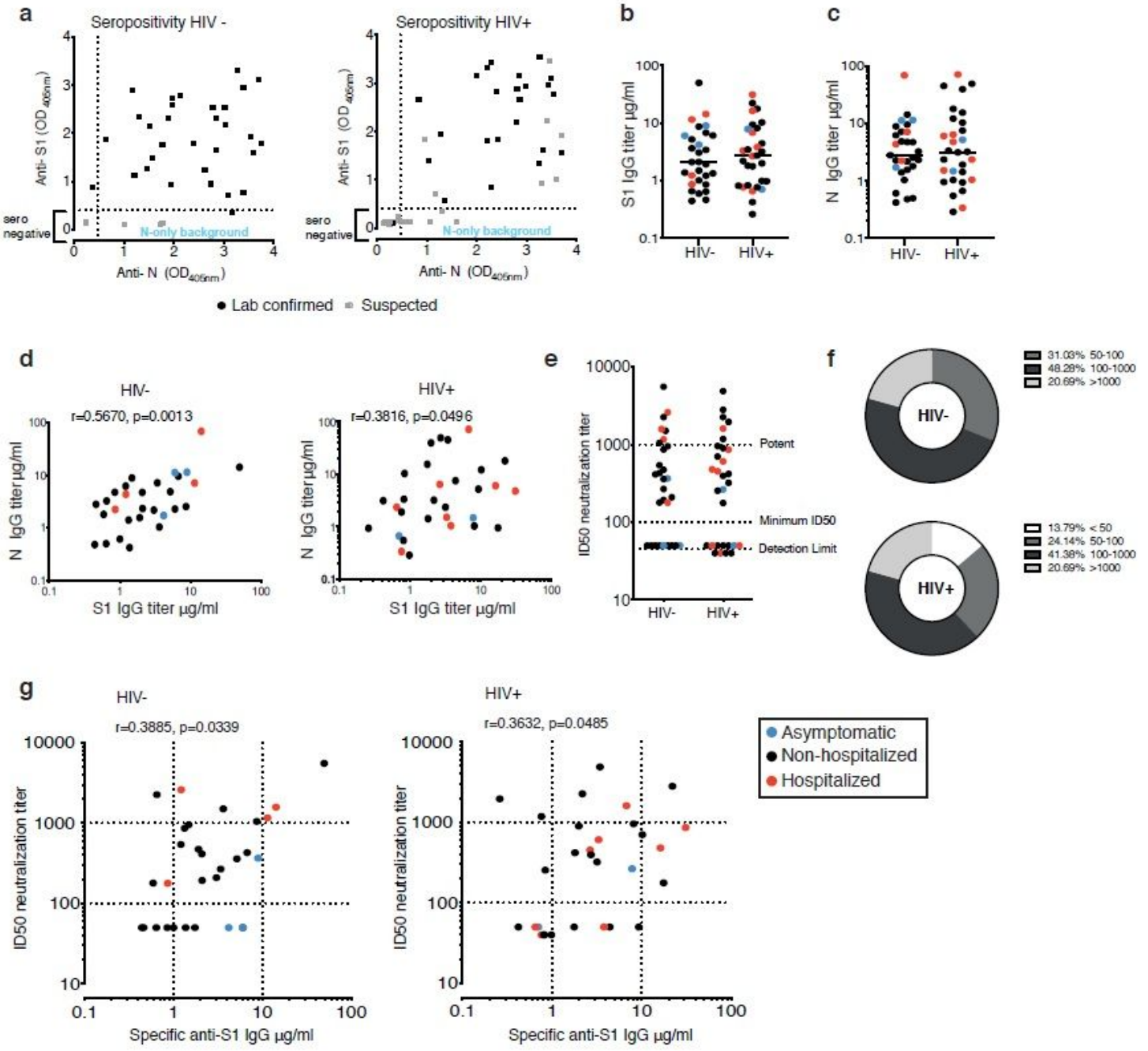

Figure 1

Antibody response in HIV positive and negative donors 642 recovered from COVID-19 disease. a Seropositivity screen of plasma samples for antibodies against the external Spike antigen, using a recombinant Spike S11-530 subunit protein (S1), and against the full-length internal Nucleoprotein (N) antigen to confirm prior infection in HIV negative and positive donors. A sample absorbance greater than 4-fold above the average background of the assay was regarded as positive. Black dots denote laboratory confirmed cases and grey dots suspected/household contacts. b Comparison of S1 IgG and N IgG antibody titers in HIV negative and c HIV positive donors. Red dots: hospitalized cases; Black dots: mild

(non-hospitalized cases); blue dots: asymptomatic cases. d Correlation between S1 IgG and N IgG titers in HIV negative and positive donors. e Neutralization titers in HIV negative and positive donors. Dotted lines indicate detection limit, minimum ID50 and potent levels >1000. f Proportion of HIV negative and positive donors with neutralizing antibodies within the given ranges. g Correlation between S1 IgG titers and neutralization titers in HIV negative and positive donors. The non-parametric Spearman test was used for correlation analysis. *p < 0.05, **p<0.01

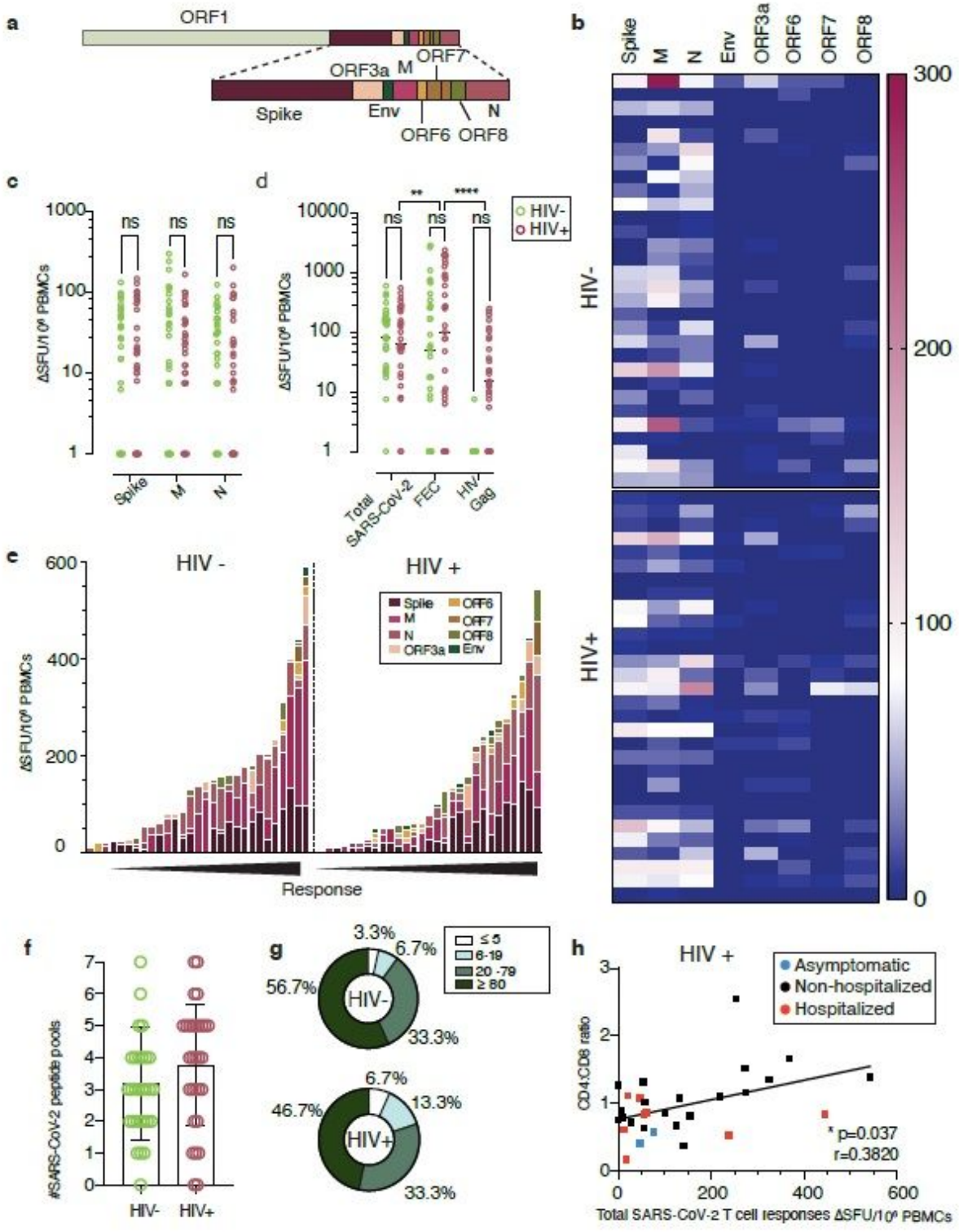

Figure 2

Similar SARS-CoV-2 specific T cell responses by IFN-γ-ELISpot in HIV positive and negative donors. a Genome organization of SARS-CoV-2 b Dominance of the IFN-γ-ELISpot responses. Heatmap depicting the magnitude of the IFN-γ-ELISpot responses to the different SARS-CoV-2 peptide pools in HIV negative and HIV positive individuals. (n=30 in each group) c Magnitude of the IFN- γ-ELISpot responses. IFN-γ SFU/106 PBMCs are shown for SARS-CoV-2 Spike (S), Membrane (M) and Nucleocapsid (N) between HIV negative (green) and HIV positive (red). (n=30 per group). d Magnitude of the IFN-γ-ELISpot responses for Total SARS-CoV-2 responses (S, M, N, ORF3a, ORF6, ORF7, ORF8 and Env), FEC and HIV Gag between HIV negative (green) and HIV positive (red). (n=30 per group). e Hierarchy of the IFNγ-ELISpot responses. IFN-γ SFU/106 PBMCs responses in order of magnitude within each group with pools each of the donors has shown positive responses in the IFN-γ-ELISpot assay. The total of SARS-CoV-2 pools tested was 7. g Proportion of T cell response magnitude in the HIV negative and HIV positive individuals. h Correlation between CD4:CD8 ratio in HIV infected individuals with their total SARS-CoV-2 responses, depicting disease severity per each donor (Red dots: hospitalized cases; Black dots: non-hospitalized cases; blue dots: asymptomatic cases.). The non parametric Spearman test was used for correlation analysis. Two-way ANOVA was used for groups comparison. *$p < 0.05$, **$p<0.01$.

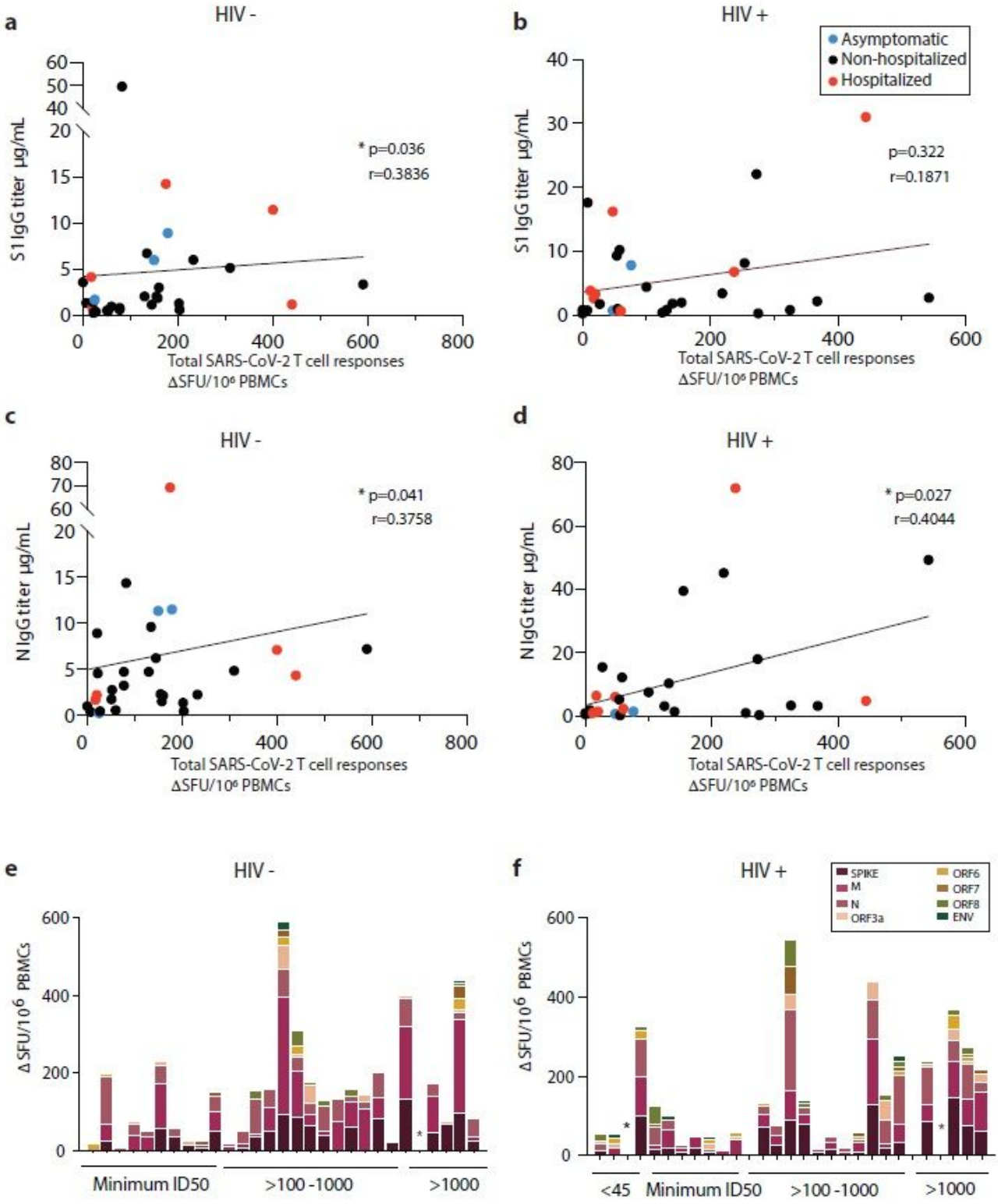

Figure 3

Interrelations between T cell and antibody responses in HIV positive and negative donors. a Correlation of total SARS-CoV-2 responses with S1 IgG titers in HIV negative and b HIV positive. c Correlation of total SARS-CoV-2 responses with N IgG titers in HIV negative and d HIV positive subjects. Red dots: hospitalized cases; Black dots: non-hospitalized cases. e Hierarchy of the T cell responses ordered by the

neutralizing capacity by their antibody titers for HIV negative and f HIV positive donors. The non-parametric Spearman test was used for correlation analysis. *p < 0.05, **p<0.01

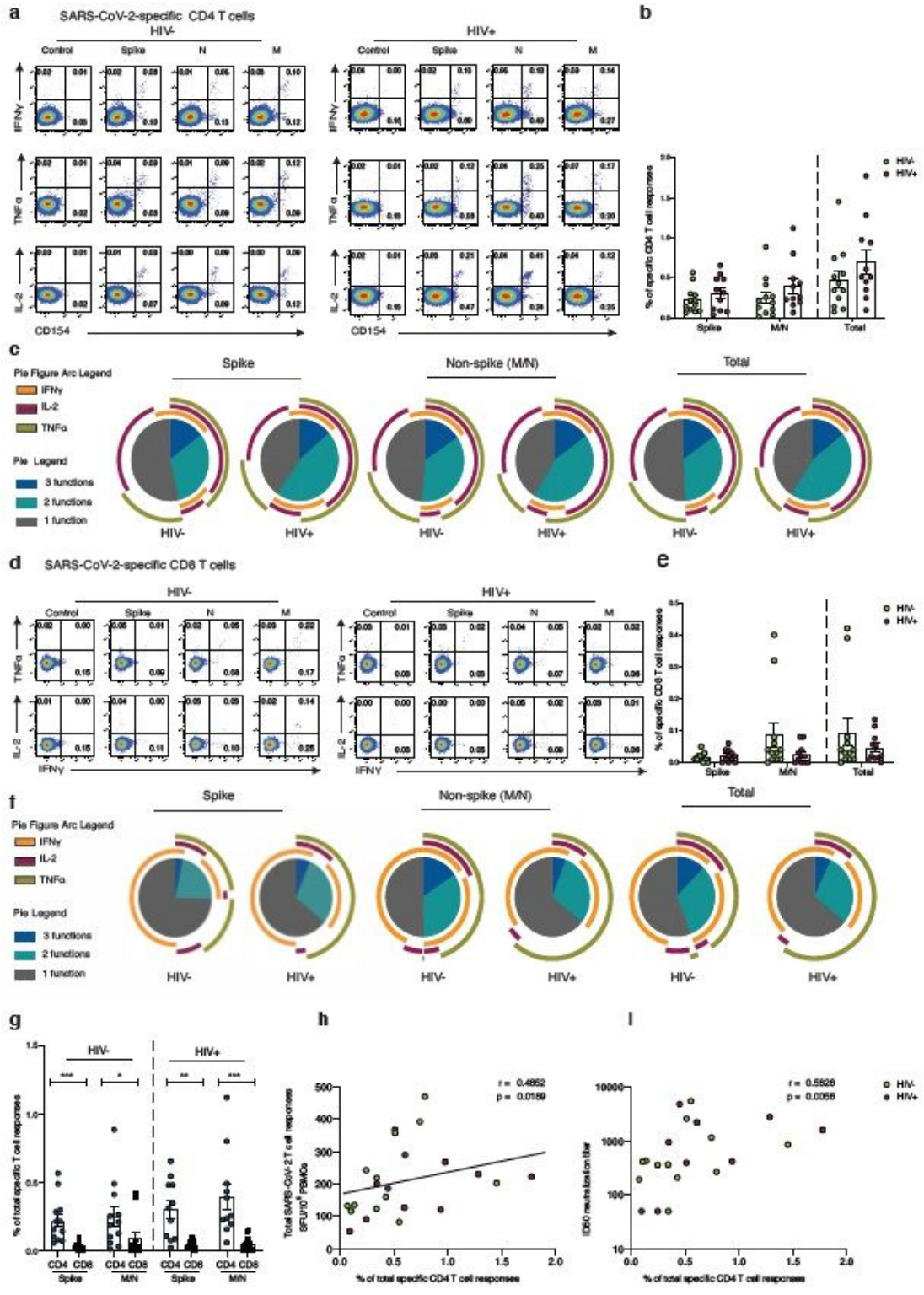

Figure 4

Composition of SARS-CoV-2-specific T cells in convalescent 687 HIV negative and HIV positive individuals. Intracellular cytokine staining (ICS) was performed to detect cytokine-producing T cells to the indicated peptide pools in HIV negative (HIV-, n=12) and HIV positive individuals (HIV+, n=11). a

Representative flow cytometric plots for the identification of antigen-specific CD4 T cells based on double expressions (CD154+IFN-g+, CD154+IL-2+, and CD154+TNF-α+) following 6-hour stimulation media alone (control) or overlapping SARS-CoV-2 peptides against Spike pool 1 and 2 (Spike), nucleoprotein (N), and membrane protein (M) directly ex vivo. b Frequency of aggregated CD4 T cell responses (CD154+IFN-g+, CD154+IL-2+, and CD154+TNF-α+) against Spike, M/N or combined (Spike and M/N) peptide pools. c Pie charts representing the relative proportions of Spike, M/N, or total (combined Spike and M/N) CD4 T cell responses for one (grey), two (green) or three (dark blue) cytokines, and pie arcs denoting IFN-γ, TNF-α and IL-2. d Representative flow cytometric plots for the identification of antigen-specific CD8 T cells based on the expression of (IFN-g+, TNF-α+, and IL-2+) against the specified peptide pools or media alone (control). e Proportion of aggregated CD8 T cell responses against Spike, M/N or combined (Spike and M/N) responses. f Pie charts representing the relative proportions of Spike, M/N and combined CD8 T cell responses for one (grey), two (green) or three (dark blue) cytokines, and pie arcs showing IFN-γ, TNF-α and IL-2. g Comparison of the frequencies of summed SARS-CoV-2- specific CD4 and CD8 T cell responses against Spike and M/N proteins. h Correlation between the frequency of total SARS-CoV-2 specific-CD4 T cells and overall T cell responses detected by IFN-γ ELISpot responses or i ID50 neutralization titer (log10) in HIV negative and HIV positive individuals. Error bars represent SEM. The non-parametric Spearman test was used for correlation analysis; p values for individual correlation analysis within groups, HIV- (green) or HIV+(red) or combined correlation analysis (black) are presented. Significance determined by Mann-Whitney U test or Wilcoxon matched- pairs signed rank test, *$p<0.05$, **$p<0.01$, ***$p < 0.001$. SPICE (simplified presentation of incredibly complex evaluations) was used for polyfunctional analysis.

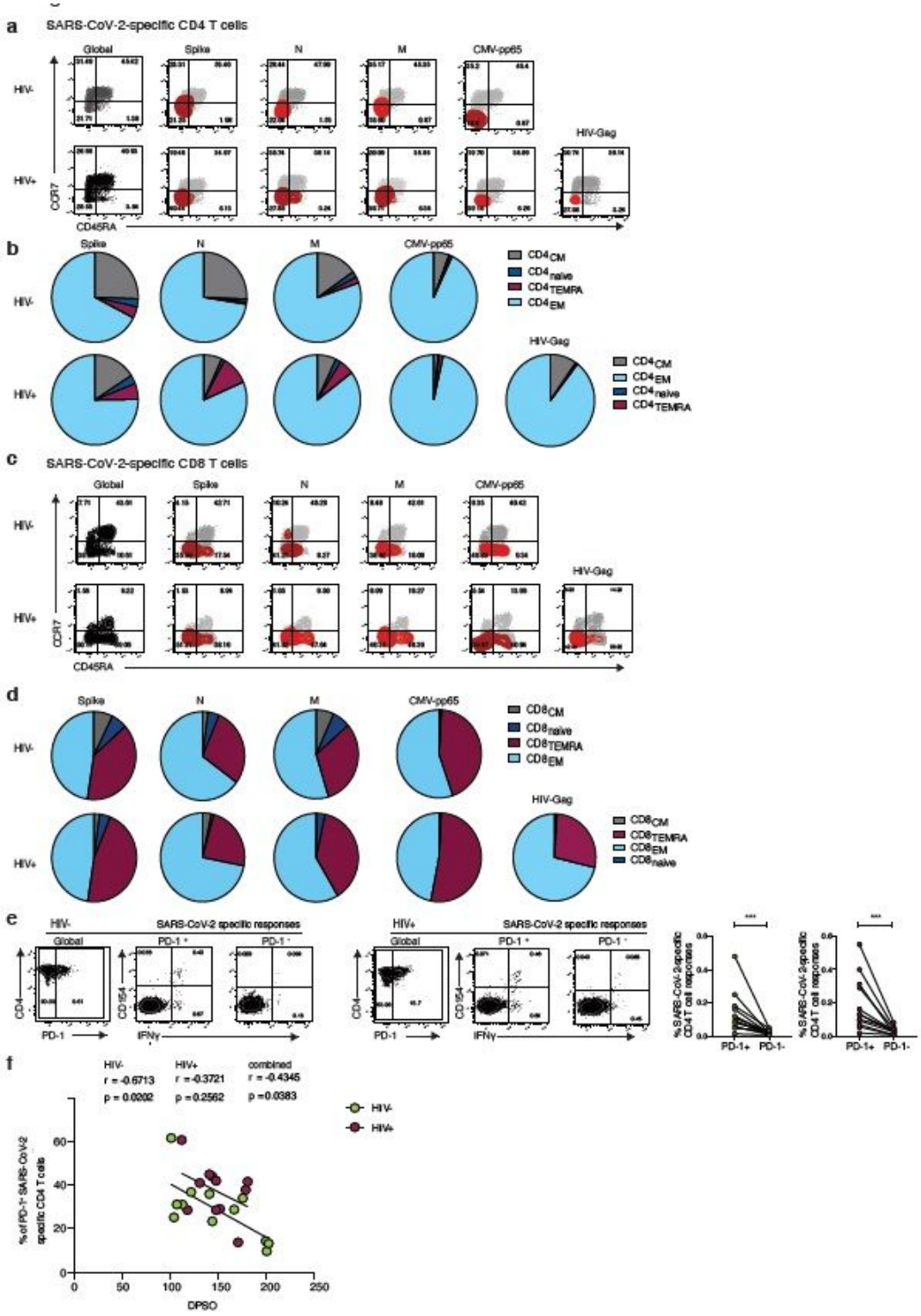

Figure 5

Phenotypic characterization of SARS-CoV-2-specific CD4 and CD8 T cells from convalescent HIV negative and HIV positive subjects. a Representative flow plots and b pie charts representing proportion of antigen-specific CD4 T cell with a CD45RA-/CCR7+ central memory (CM), CD45RA+/CCR7+ naïve, CD45RA+/CCR7- terminally differentiated effector memory (TEMRA) and CD45RA-/CCR7- effector memory (EM) phenotype from HIV negative (HIV-, n=12) and HIV positive individuals (HIV+, n=11)

against SARS-CoV-2 Spike, M, N, CMV pp65 and HIV gag. c Representative flow plots and d pie charts representing proportion of CD45RA-/CCR7+ central memory (CM), CD45RA+/CCR7+ naïve, CD45RA+/CCR7- terminally differentiated effector memory (TEMRA) and CD45RA-/CCR7- effector memory (EM) antigen-specific CD8 T cell subsets against SARS-CoV-2 Spike, M, N, CMV pp65 and HIV gag. e Representative flow plots from an HIV negative donor (HIV-) and an HIV positive donor (HIV+) showing expression of CD154 and IFN-g production from PD1+ and PD1- SARS-CoV-2-specific CD4 T cells and paired analysis of responses in HIV negative (HIV- , n=12) and HIV positive (HIV+, n=11) individuals. f Correlation between frequency of (PD- 1+CD154+IFN-g+ SARS-CoV-2-specific CD4 T cells and DPSO in both groups. Significance determined by Wilcoxon matched-pairs signed rank test, *p<0.05, **p<0.01, ***p < 0.001. The non-parametric Spearman test was used for correlation analysis; p values for individual correlation analysis within groups, HIV-, HIV+, or combined correlation analysis (black) are presented.

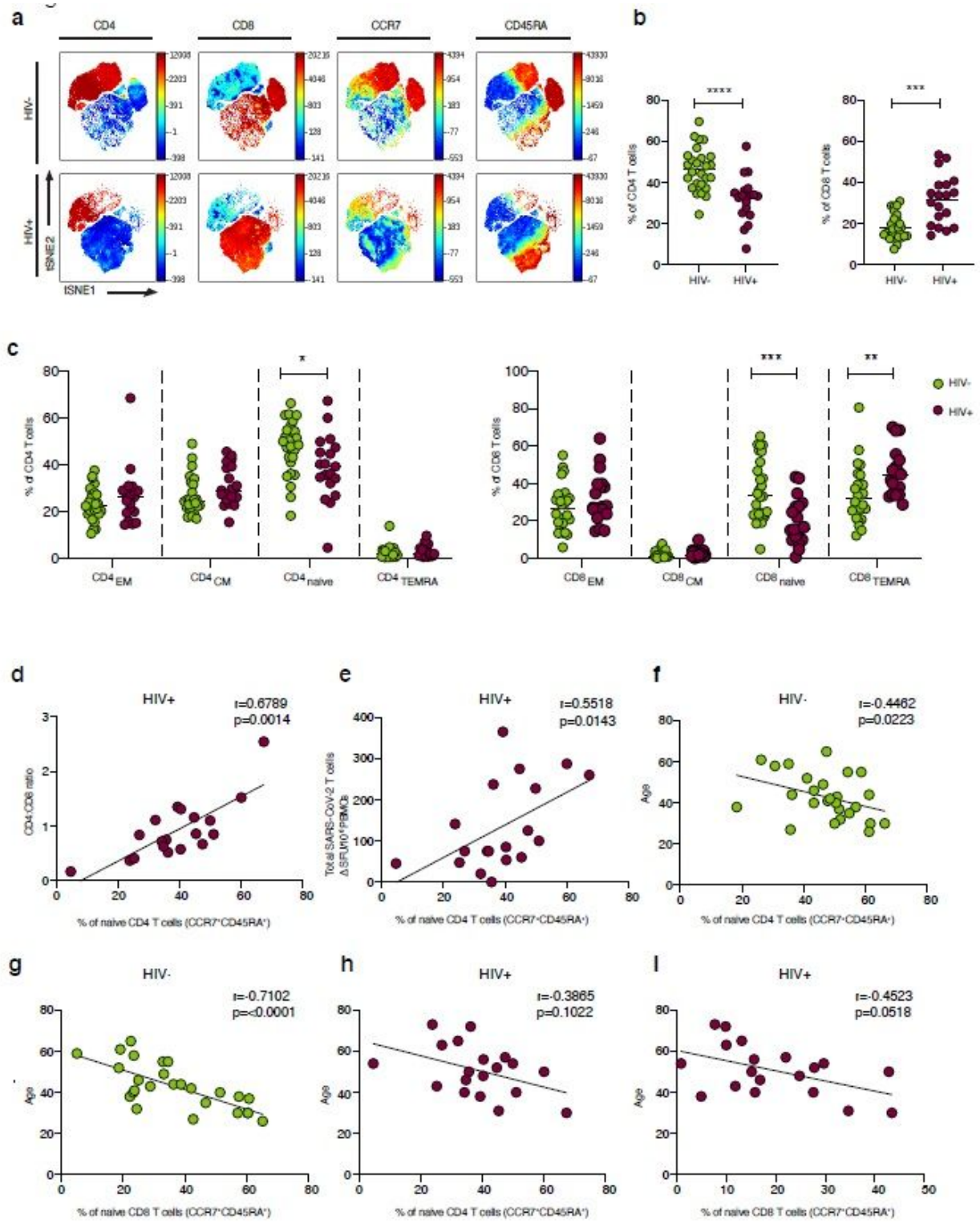

Figure 6

Immune profile relationships between convalescent HIV 733 positive and negative individuals. a viSNE analysis of CD3 T cells in HIV negative (top panel) and HIV positive donors (lower panel). Each point on the high-dimensional mapping represents an individual cell and colour intensity represents expression of selected markers. b Frequency of CD4 and CD8 T cells out of total lymphocytes in SARS-CoV-2 convalescent HIV negative (HIV-, n=26) and HIV positive individuals (HIV+, n=19) via traditional gating. c

Summary data of the proportion of CD45RA- /CCR7+ central memory (CM), CD45RA+/CCR7+ naïve, CD45RA+/CCR7- terminally differentiated effector memory (TEMRA) and CD45RA-/CCR7- effector memory (EM) CD4 and CD8 T cell subsets it the study groups. d Correlation between CD4:CD8 ratio and frequency of naïve CD4 T cells in HIV-positive individuals. e Correlation between frequency of naïve CD4 T cells and total SARS-CoV-2 T cell responses, detected via ELISpot, in HIV positive individuals. f Correlation between frequency of naïve CD4 T cells and g naïve CD8 T cells and age in HIV negative individuals. h Correlation between frequency of naïve CD4 T cells and i naïve CD8 T cells age in HIV positive donors. Significance determined by Mann-Whitney test, *p<0.05, **p<0.01, ***p < 0.001. The non-parametric Spearman test was used for correlation analysis.

Supplementary Files

This is a list of supplementary files associated with this preprint. Click to download.

- Supplementarymaterial.pdf